Design of an Optical Box for Laser Doppler Anemometer Measurements

By

Long Zulkarnaen Bin Long Zainudin

Submitted to the Mechanical Engineering Department
In partial fulfillment of the requirement for the
Bachelor of engineering (Hons)
(Mechanical Engineering)

MAY 2011

Universiti Teknologi PETRONAS
Bandar Seri Iskandar
31750 Tronoh
Perak Darul Ridzuan

CERTIFICATION OF APPROVAL

Design of an Optical Box for Laser Doppler Anemometer Measurements

by

Long Zulkarnaen Bin Long Zainudin

A report submitted to the
Mechanical Engineering Department
Universiti Teknologi PETRONAS
In partial fulfillment of the requirement for the
Bachelor of engineering (Hons)
(Mechanical Engineering)

Approved by,

(Dr.Azuraien Japper@Jaafar)
Project Supervisor

UNIVERSITI TEKNOLOGI PETRONAS

TRONOH, PERAK

MAY 2011

CERTIFICATION OF ORIGINALITY

This is to certify that I am responsible for the work submitted in this project, that the original work is my own except as specified in the references and acknowledgements, and that the original work contained herein have not been undertaken or done by unspecified sources or persons.

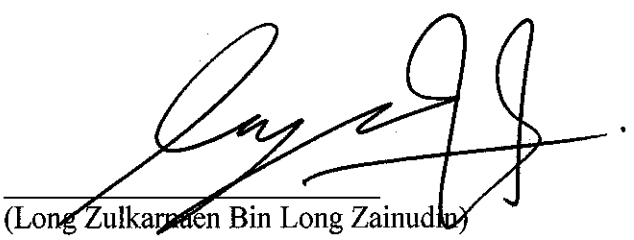

(Long Zulkarnaen Bin Long Zainudin)

ABSTRACT

This report is about **Design of an optical box for Laser Doppler Anemometer measurements and fluid velocity measurement using Laser Doppler Anemometer.** Laser Doppler Anemometer uses a beam of light from laser to measure velocity of fluid flows. The objective of the project is to design a module of laser Doppler anemometer that can simplify mathematical derivation for refraction correction of velocity measurement and to run a test on the test section to obtain transversal measurement of fluid velocity very close to the pipe wall. The main factor to be considered in the experiment is the refractive index of the elements used. The design will include acrylic pipe tube with '+' cross slit on the pipe wall, Teflon film to cover the cross slit, a gear, and a connecting device to connect the test section to the pipe section. The pipe needs to be rotatable so that it can be used to measure the velocity of fluid flow at different points. The experiments will be conducted using LDA laser which will pass through different types of medium before reaching the fluid interface. Mathematical derivation can be simplified by having the optical box and a cross slit on the pipe wall, which will reduce refraction as the beams goes through the box, fluid inside the box and straight to the fluid inside the pipe by eliminating the effect of pipe curvature. For that, refraction needs to be as small as possible in such way that angle of incident is almost the same with angle of refraction (zero refraction), where the refractive index of the pipe wall and the Teflon film covering the slit are similar to the fluid being tested.

ACKNOWLEDGEMENTS

This final year project would not have been possible without the guidance and the help of several individuals who in one way or another contributed and extended their valuable assistance in the preparation and completion of this study. First and foremost, my utmost gratitude to my supervisor Dr Azuraien Jaafar@Japper for the continuous support for my final year project, for her patience, motivation, enthusiasm, and immense knowledge. Her guidance helped me in all the time of research and writing of this final report. I could not have imagined having a better supervisor and mentor for my final year project. Besides my supervisor, I would like to thank Mr Azman from Universiti Sains Malaysia (USM) for his assistance on completing this project and providing necessary information. Engineering students who in one way or another were helps in giving assistance to understand the physics part of my project. Last but not the least, I would like to thank my family for giving birth to me at the first place and supporting me spiritually throughout my life and the one above all of us Allah for answering my prayers and giving me the strength to complete my final year project.

TABLE OF CONTENT

LIST OF FIGURES

LIST OF TABLES

CHAPTER 1
INTRODUCTION

1.1 Background study

The basic idea of this project is to design an optical box for Laser Doppler Anemometer and conduct experiments on it to obtain data for fluid velocity measurement. The pipe system consists of pump, manometer, flow meter, pipe, transducer, damper, frequency regulator, tank and fittings as shown in the picture below. The design of the circular pipe-flow facility consisted of a small open cross slit that allow laser beam to go through it without any refraction. Teflon film is used to cover the cross slit to minimize the refraction of the laser beam. The circular pipe is rotatable to allow measurements at different points within the circular pipe. A flat square box is constructed around the pipe to hold the fluid stationary in the outer region of the slit and to minimize the refraction of the laser beam. A thin film at the cross slit will also be used to prevent water from the box to mix and interfering the flow of fluid inside the pipe. It is mainly used to minimize refraction of the laser beam. The designed module is attached to the test section at a point where the fluid is in fully-developed condition. Software that is used for the design project is CATIA V5R12. The experiment will be conducted in re-circulatory pipe flow facility that will be constructed by another FYP student.

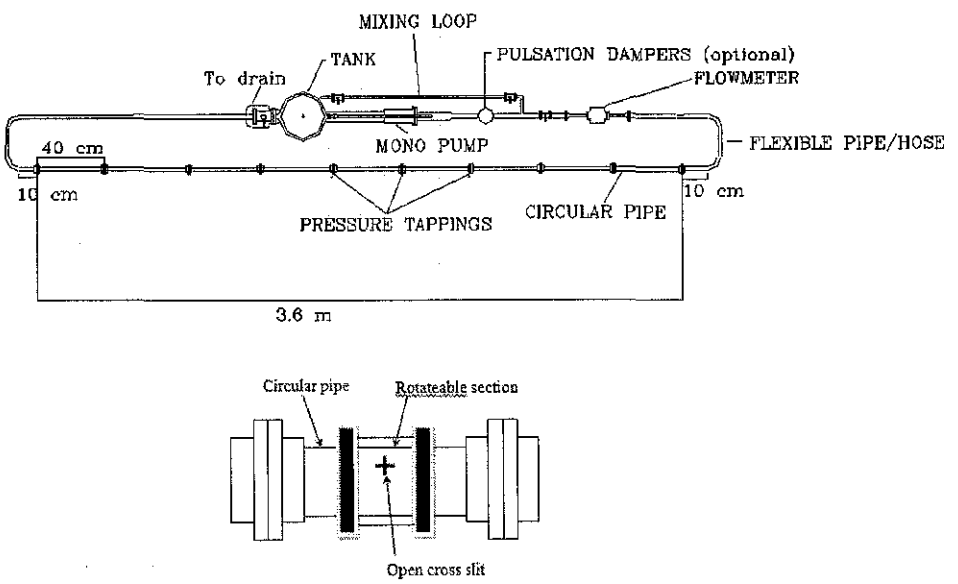

Figure 1.1: Pipe flow rig and test section module with cross slit

1.2 Problem Statement

Laser Doppler Anemometer (LDA) is a technology used to measure velocities of flows or more specifically velocities of small particles in fluid flows. It is being recognized mainly for its non-intrusivity, directional sensitivity and zero calibration requirements. One of the difficulties in LDA measurement is to obtain transversal measurements very close the wall, in channel or pipe flow. Numerical solutions have been developed to correct this problem but it requires long mathematical derivation. Two velocity component, radial, v', and tangential, w', velocities, need to be measured to determine Reynolds shear stress, and hence requiring the horizontal and vertical beams to coincide with each other at the measuring volume. Presence of curved wall in circular pipe changes the optical path of the vertical beam, and causes it not to coincide with each other. This cause difficulty in obtaining data to measure Reynolds shear stress ($\rho u'v'$). This project is to improvise the existing method to make it as simple as possible to get the measurement of fluid velocity that require simple mathematical correction but yet allows accurate measurement of two velocity component inside the cylindrical pipe.

1.3 Objective

The objectives of this project are:

- To study and understand the concept of laser Doppler anemometer (LDA).
- To design a module or "optical box" for laser Doppler anemometry measurements.
- To search for possible types of thin film that can be used within the optical box to minimize laser beam refraction for the experiment.

CHAPTER 2
LITERATURE REVIEW

2.1 Overview

Laser Doppler anemometers use beam of light from a laser that is split into two beams, with one transmitted out of the anemometer. When the particles are in great motion, they produce a Doppler shift for measuring air speed in the laser light, which is used to calculate the speed of the particles, and therefore the air around the anemometer. The technique is based on the measurement of laser light scattered by particles that pass through a series of interference fringes (a pattern of light and dark surfaces). The scattered laser light oscillates with a specific frequency that is related to the velocity of the particles. Laser light will be refracted as it goes from one medium to another medium with different refractive index. To avoid large refraction in this experiment, a thin fim made by Teflon will be used as a medium to separate fluid in the square box and fluid in the circular pipe. The laser light will pass through transparent square box and goes to the stationary fluid before reaching the Teflon film and fluid in the circular pipe. The important thing is to reduce refraction of the laser beam so that vertical and horizontal beams for two-component measurements (Reynolds shear stress) will coincide.

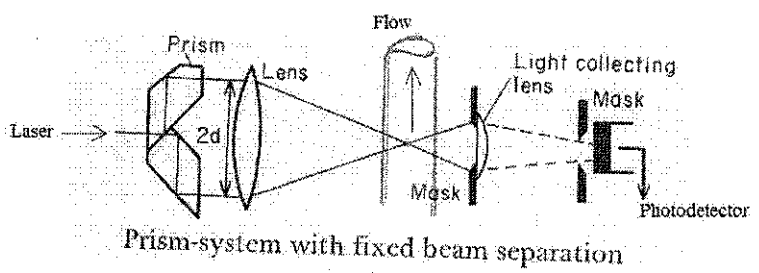

Figure 2.1.1: Typical Laser Doppler anemometer

Beams from the laser are split into two parts which are necessary to provide interference in the local region of the flow where velocity measurements are required. Part of the volume of interference is observed by a light collecting system and imaged on a photo

detector. The photo detector converts the optical signal to an electronic signal which is processed by an appropriate signal-processing arrangement.

2.2 Previous method of LDA measurements through curved pipe wall

In the past years, several techniques were developed to overcome the refraction problem across a curved pipe wall. Presence of curved wall in circular pipe changes the optical path of the vertical beam, and causes it not to coincide with each other. Herman Z Cummins and Y. Yeh have invented the Laser Doppler Anemometer in 1964. The anemometer was produced during the team's research of fluid mechanics while working at Columbia University. During the experiments for measurements of internal flows, some problems are encountered. One of it is the difficulty in obtaining transversal measurements very close the wall, in channel or pipe flow. Numerical solutions have been developed to correct this problem but it requires long mathematical derivation. Two velocity component, radial, v', and tangential, w', velocities, need to be measured to determine Reynolds shear stress, and hence requiring the horizontal and vertical beams to coincide with each other at the measuring volume.

Previously, many researches have been conducted using LDA to obtain measurement of fluid velocity. One of the researches has been carried out by Wei and Willmarth (1989) that proposed the use of a channel supplied with closed circuit and a complex measuring station. The laser beams entered the test section through a slot covered with a thin window of heat shrink Mylar film. To minimize the beam refraction, an optical head made up of two glass window mounted in a triangular brass chamber was used. In order to balance the pressure exerted on the Mylar film by the water in the test section, the false head was connected to both the test section and the optical head. The diaphragm in the false head was predisposed to transmit the same pressure from the test section to the optical head.

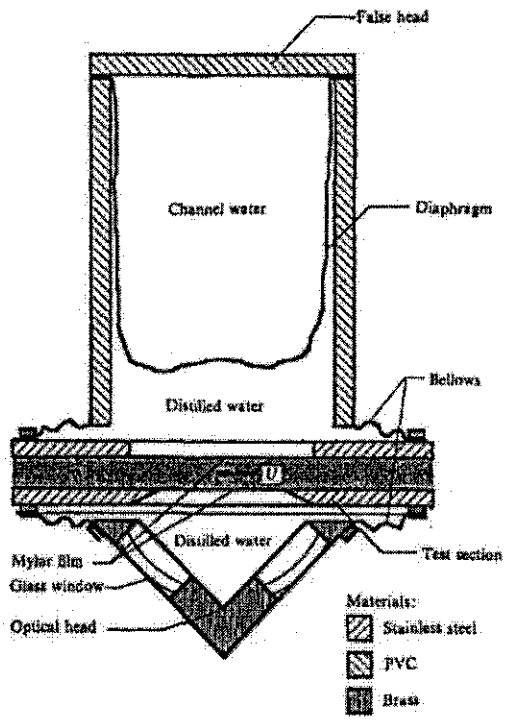

Figure 2.2.1: Test section built by Wei and Willmarth

Den Toonder and Nieuwstadt (1997) have developed a test section containing a perspex box and thin foil made up from Teflon FEP replacing the pipe wall to measure turbulent flows. Error at the test section occurred in this experiment when measurement was taken very close the wall due to the reflections of the laser beam from the pipe wall which was picked up by the receiving optics resulting in an inaccurate data. The authors also conclude that turbulence statistics is dependent on Reynolds number (Re). Their results show that turbulence statistics scaled on inner variables are Reynolds-number dependent in some range of Reynolds numbers. As Re increases, the scaled quantities approached an asymptotic value.

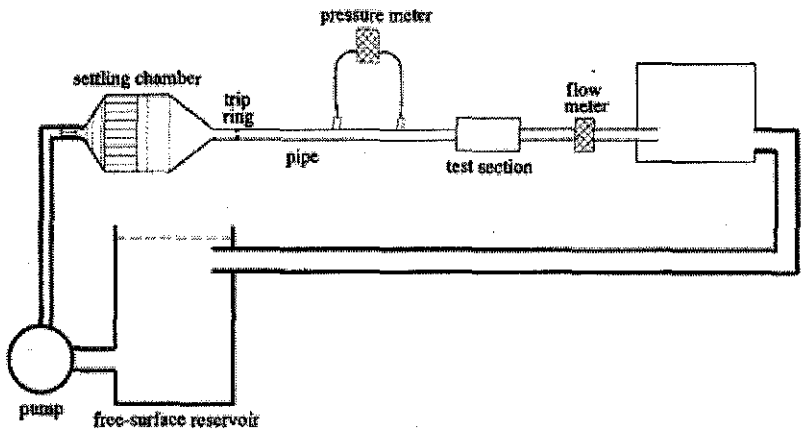

The pipe flow facility. The main part is a cylindrical perspex pipe with length 34 m and inner diameter 40 mm. It contains a test section for the LDV measurements.

Figure 2.2.2: Pipe flow rig by Den Toonder and Nieuwstadt

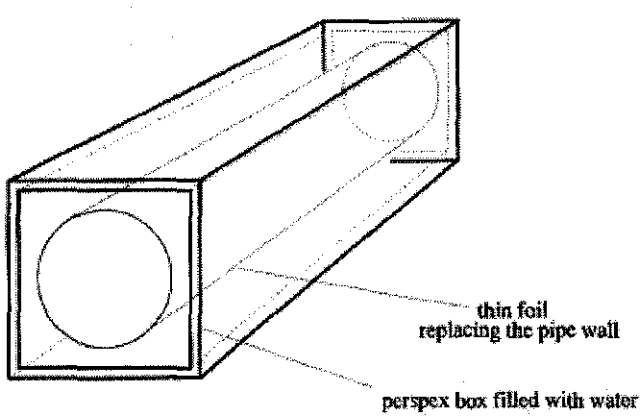

Figure 2.2.3: Test section by Den Toonder and Nieuwstadt

Poggi et. al. (2002) performed near-wall measurements using LDA have proposed new technique of near wall region of turbulent channel flows with LDA. The method employs a very narrow slot in the channel bottom which allows the passage of the laser beam without changing their path, providing high quality measurement very close to the wall. They found the agreement between the measured statistics of the streamwise and vertical velocity components and the more recent literature data testify the validity of the proposed experimental solution. This technique proposed the use of

different material for the test section, which is Plexiglass sheet with a narrow and small cut filled with water and covered by Teflon FEP, to allow only the vertical laser beam pass through it. This method is very simple to use and allows experimental investigations without requiring extensive mathematical derivation. It can also be used in other flow situations, such as rotating flow and flow at rough walls.

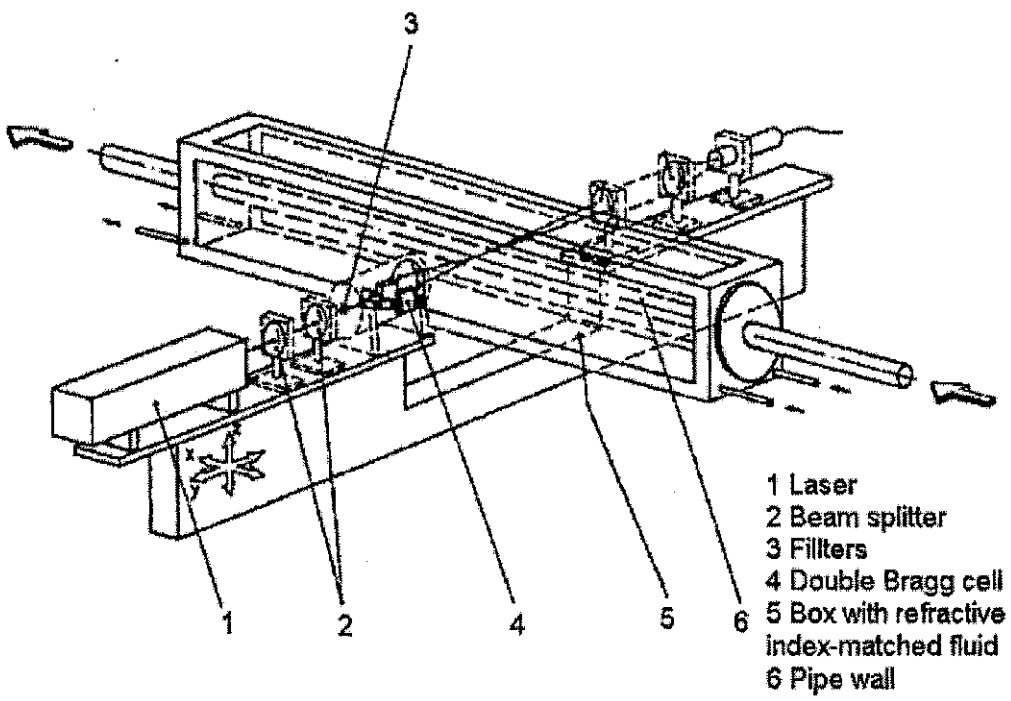

Figure 2.2.4 Test section by Poggi et. al.

2.3 Refraction

When an ultrasonic wave passes through an interface between two materials which have different refractive index at some angle the waves are both reflected and refracted..This also occurs with light, which is why objects seen across an interface appear to be shifted away or closer relative to where they really are. Refraction takes place at an interface due to the different velocities of the acoustic waves within the two materials. The velocity of sound in each material is determined by the material properties (elastic modulus and density) for that material. The wave tend to bend because portion of the wave in the second material is moving faster than in the first material. This law of refraction can be described by Snell's law.

Snell's Law describes the relationship between the angles and the velocities of the waves. It equates the ratio of material velocities V_1 and V_2 to the ratio of the Sine's of incident ($theta_1$) and refracted ($theta_2$) angles, as shown in the following equation:

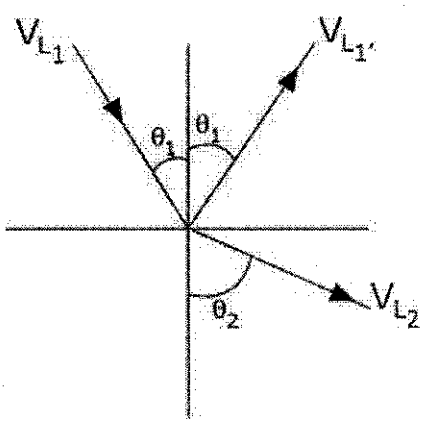

$$\frac{\sin\theta_1}{\sin\theta_2} = \frac{v_1}{v_2} = \frac{n_2}{n_1} \qquad (1)$$

v = velocity, SI units are m/s

n = refractive index, which is unitless

V_{L1} is the longitudinal wave velocity in material 1.

V_{L2} is the longitudinal wave velocity in material 2.

Note that in the diagram, there is a reflected longitudinal wave ($V_{L1'}$) shown. This wave is reflected at the same angle as the incident wave because the two waves are traveling in the same material, and hence have the same velocities.

2.4 Refraction Correction for LDA measurement

In the experiment of Laser Doppler Anemometer, there are some corrections of refraction for cylindrical surface that need to be performed in order to calculate the velocity component of the fluid flow inside the pipe. The fluid velocity is measured based on the frequency of light pulses emitted from particles in the fluid as they pass through a zone of interference fringes produced by intersection of two beams. There are many methods for refraction correction of LDA but nothing proved to be the most accurate one. Figure 2.4.1 shows the laser beam orientation and traversing direction for axial, tangential, and radial measurement in ideal situation (without refraction).

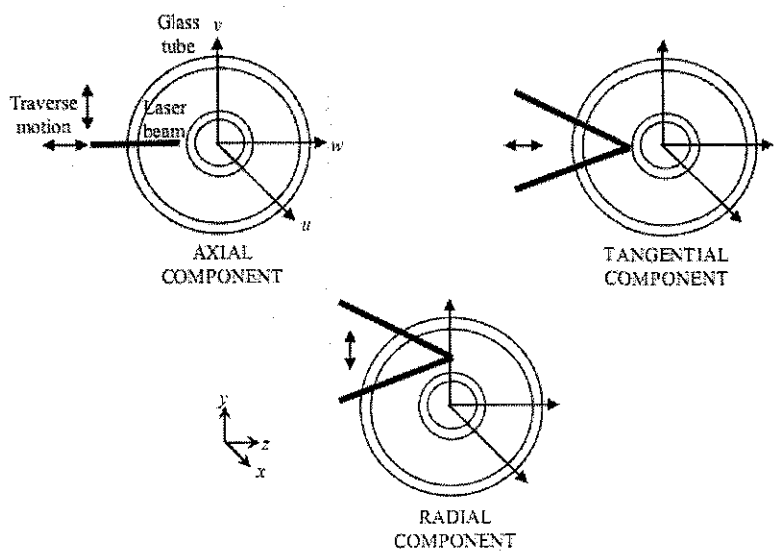

Figure 2.4.1: Laser beam orientation and traversing direction for axial, tangential, and radial measurement

Method introduced by John D. Boadway and Emin Karahan (1981) stated that Laser Doppler Anemometer measures fluid velocity by determining the frequency of oscillation of light pulses emitted from particles in the fluid as they pass through a zone of interference fringes produced by intersection of two beams.

$$v = \frac{f_D \lambda}{2\sin\left(\frac{\theta}{2}\right)} \tag{2}$$

Where,

$v = fluid\ velocity\ (\frac{m}{s})$

$f_D = Doppler\ frequency\ (\frac{cycles}{second})$

$\lambda = wavelength\ (m)$

$\theta = angle\ between\ the\ laser\ beam$

For this experiment, there are three velocity components involve for the calculation of Reynolds Shear Stress which are axial, tangential, and radial velocity component.

$$Reynold\ Shear\ Stress = \rho u'v' \tag{3}$$

Where

$u' = Axial\ velocity$

$v' = Radial\ velocity$

Because of the cylindrical geometry, the corrections factor for fluid velocity need to be taken into account and it is derived from the Snell's law of refraction regarding the relationship between the real refracted position of beam intersection and the virtual position without refraction.

Axial velocity measurement (u')

For axial velocity measurement, the optical system should be oriented such that the plane containing the beam passes through the cylindrical axis and the bisector between the beams at right angle to the axis. The refracting surface will be perpendicular to the beam bisector as with the pipe plane. The intersection point is moved along a diameter on which the bisector lies and it can be calculated using the equation below with an assumption that, since the half angles are very small, their sine and tangent are approximately equal.

$$X_f = \eta_f X_a - \frac{\eta_f}{\eta_w}.t \tag{4}$$

Where

$X_f = Distance\ of\ the\ real\ beam\ intersection\ from\ the\ inside\ of\ the\ curved\ pipe$
$X_a = Distance\ of\ the\ virtual\ intersection,\ assuming\ no\ refraction,$
$from\ outside\ of\ the\ curved\ pipe$
$\eta_f = Index\ of\ refraction\ of\ the\ fluid$
$\eta_w = Index\ of\ refraction\ of\ the\ circular\ pipe$
$t = thickness\ of\ the\ pipe$

For calculation of axial velocity, equation 1 may be applied for direct calculation using the wavelength in air and the unrefracted angle since there should only be refraction in the axial direction.

Tangential velocity measurement (w')

For tangential velocity measurement, the optical system should be oriented such that the bisector between the beams is perpendicular and passes through the axis of the cylinder with a plane containing both beams perpendicular to the axis. The point of intersection is moved along the diameter nearer to the optical system on which the bisector lies and the curvature of the pipe cylinder will make it act as a convex lens thus increasing the angle of the beam. The refraction correction factor can be calculated with an assumption that the sine and tangent for the small angle are approximately the same.

$$G = \eta_f \left\{ 1 + \left(\frac{r_a}{R_o}\right) \cdot \left[\frac{(1-\eta_w)}{\eta_w} + \left(\frac{R_o}{R_I}\right) \cdot \frac{\left(1-\frac{\eta_f}{\eta_w}\right)}{\eta_f} \right] \right\} \quad (5)$$

Where

$G = Refraction\ correction\ factor, also\ known\ as\ C_f\ where\ C_f = \frac{1}{G}$
$\eta_f = Index\ of\ refraction\ of\ the\ fluid$
$\eta_w = Index\ of\ refraction\ of\ the\ circular\ pipe$

$r_a = Radius\ position\ of\ the\ virtual\ intersection\ of\ beam\ with\ no\ refraction$
$R_o = Outer\ radius\ of\ the\ pipe\ wall$
$R_I = Inner\ radius\ of\ the\ pipe\ wall$

This correction factor will be used to calculate velocity by using it as a factor as applied to equation 1 using the half angle and wavelength in air.

$$V_f = \frac{V_a}{G} \quad (6)$$

Where

$V_f = Corrected\ velocity\ in\ fluid$
$V_a = Velocity\ calculated\ from\ equation\ 1$
$r_f = \frac{r_a}{G}$ (7)

Where

$r_f = true\ radius\ position\ of\ beam\ intersection\ point$

Radial velocity measurement (v')

For radial velocity measurement, the optical system should be oriented as for tangential velocity measurement, but the point of intersection is now moved. Setting for measurement at different radius must be made by moving the optical system side-ways with respect to the axis of the cylinder pipe rather than to, or from the axis as is required for the other directions. The calculation for this arrangement is more complex from the previous two arrangements. The angle of incident of the laser beam at the wall of the cylinder may be too large to make any simplifying assumption and the series of trigonometric equations solutions are better performed using computer algorithm.

For radial velocity measurement the correction factor, G is equal to η_f, the refractive index of the fluid. To calculate the fluid velocity, V_f and true radius position, r_f of the intersection point, equation 4 and 5 may be used.

$$V_f = V_r = \frac{V_a}{G} \tag{8}$$

$$r_f = r_r = \frac{r_a}{G} \tag{9}$$

The difficulty in this arrangement is that the real bisector between the beams at the point of intersection is not a tangent to the circle but at a small angle ϕ. Because of this, the measured velocity contains a small component of tangential velocity shown in equation below.

$$V_m = V_r cos\phi + V_\theta sin\phi \tag{10}$$

Where

$V_m = Measured\ velocity$
$V_r = Radial\ velocity$
$V_\theta = Tangential\ velocity$
$\phi = Angle\ of\ bisector\ to\ a\ true\ tangent$

$$\phi = 13.1\left(\frac{r_a}{R_o}\right) + 7.75\left(\frac{r_a}{R_o}\right)^5 \tag{11}$$

This method is among the simplest method introduced for refraction correction for fluid velocity measurement but there is one problem arise from this method where it does not take into account the effect of pipe medium (acrylic) for the correction on the intersection position.

There is also another method introduced to calculate refraction correction done by A.F.Bicen (1982). He improvises the method developed by D. Boadway and Emin Karahan (1981). It stated that velocity is equal to the wavelength and the path of the laser beam, thus the half angle of the beam and the point of intersection will change if the beam goes through different medium with different refractive index.

$$v = \frac{f_D \lambda}{2\sin\left(\frac{\theta}{2}\right)} \tag{12}$$

Where,

$v = fluid\ velocity\ (\frac{m}{s})$

$f_D = Doppler\ frequency\ (\frac{cycles}{second})$

$\lambda = wavelength\ (m)$

$\theta = angle\ between\ the\ laser\ beam$

Axial velocity measurement (u')

For axial velocity measurement, the optical system should be oriented such that the plane containing the beam passes through the cylinder pipe axis with the bisector between the beams. In this experiment, it is assumed that intersection point is moved along the diameter on which the bisector lies. Refraction only occurs in the axial plane since refracting surfaces are perpendicular to the bisector. It is assumed that the sine and tangent of half angle are almost equal since they are very small.

$$x_f = n_f x_a + \underbrace{\left(1 - \frac{n_f}{n_w}\right)}_{\text{const 1}} t + \underbrace{(n_f - 1)R_o}_{\text{const 2}} \tag{13}$$

Where:

χ_f = True point of intersection with refraction

χ_a = Virtual point of intersection without refraction

n_f = fluid refractive index

n_w = wall refractive index

For axial velocity measurement, there is no correction needed for fluid velocity since correction factor is assumed to be unity, which is equal to one.

$$\boxed{\begin{aligned} V_f &= C_f V_a \\ C_f &= 1 \end{aligned}} \qquad (14)$$

C_f = Correction factor

V_f = Corrected fluid velocity

V_a = Fluid velocity from measurement

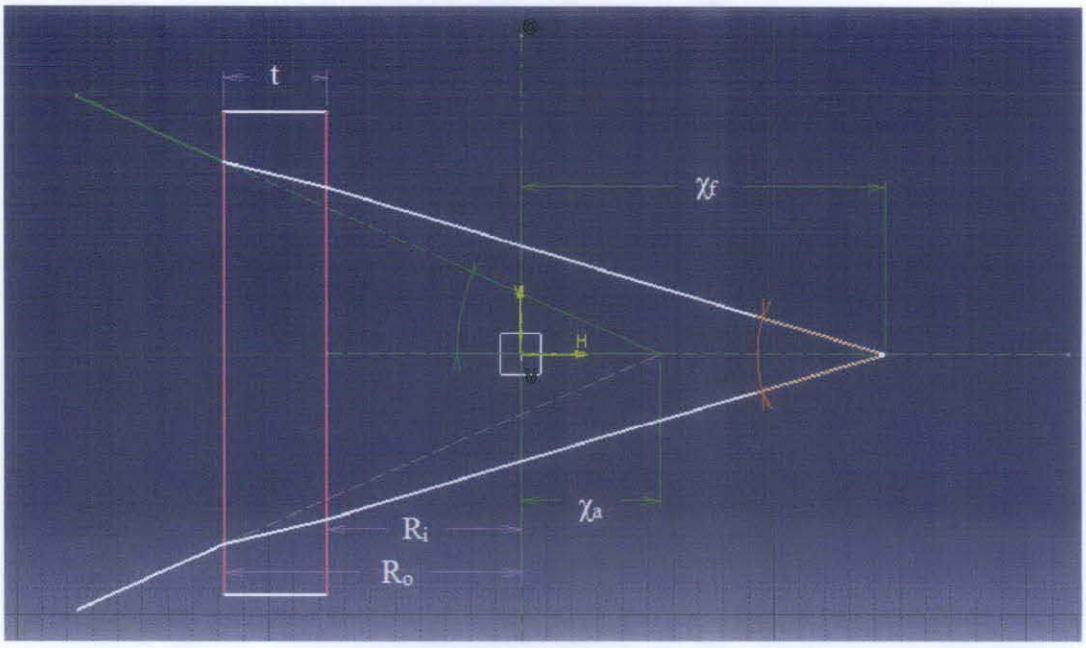

Figure 2.4.2: Refraction of laser beam during axial velocity measurement

Tangential velocity measurement (w')

For tangential velocity measurement, the optical system should be oriented such that the plane containing the beams is perpendicular to the cylindrical axis with the bisector passing through it. The point of intersection is moved along the diameter of which the bisector lies. It is assumed that the sine of small angle is equal to the sum of each individual sines.

$$C_f = \underbrace{\frac{1}{n_f}}_{\text{const 1}} \frac{1}{\left[1+\left(\frac{r_a}{R_o}\right)\left[\underbrace{\left(\frac{R_o}{R_i}\right)\frac{\left(\frac{n_f}{n_w}-1\right)}{n_f}}_{\text{const 2}} + \underbrace{\frac{n_w-1}{n_w}}_{\text{const 3}}\right]\right]}$$

$$x_f = C_f x_a$$

$$V_f = C_f V_a \qquad (15)$$

Where:

t = wall thickness

n_f = fluid refractive index

n_w = wall refractive index

R_i = inner radius

R_o = outer radius

$r_a = \chi_a$ = radius of beam intersection without refraction

$r_f = \chi_f$ = radius of beam intersection with refraction

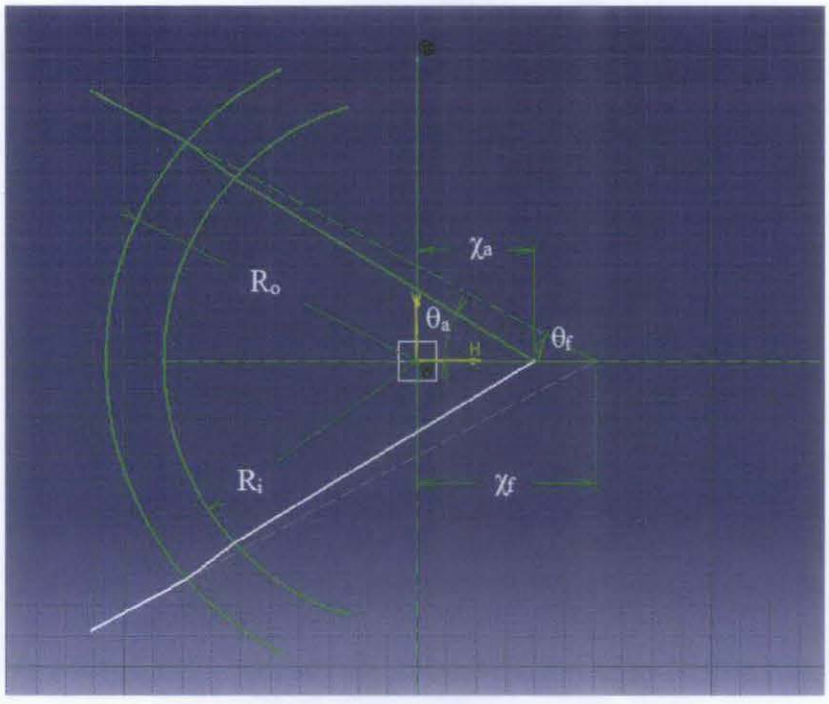

Figure 2.4.3: Refraction of laser beam during tangential velocity measurement

Radial velocity measurement (v')

For radial velocity measurement, the optical system should be oriented such that the plane containing the beam is radial to cylinder axis and the point of intersection is moved along the orthogonal diameter which is at right angles to the unrefracted beam bisector. However, the true point of intersection will not lie on the orthogonal diameter, but it lays on the inclined of the diameter by an angle of ϕ_f.

$$
\begin{aligned}
C_f &= \frac{1}{n_f} \\
x_f &= C_f x_a \\
V_f &= C_f V_a \\
\phi_f &= \underbrace{\sin^{-1}\left(\frac{x_a}{n_w R_i}\cos\theta_a\right)}_{\text{const 1}} - \underbrace{\sin^{-1}\left(\frac{x_a}{n_w R_o}\cos\theta_a\right)}_{\text{const 2}} \\
&\quad - \underbrace{\sin^{-1}\left(\frac{x_a}{n_f R_i}\cos\theta_a\right)}_{\text{const 3}} + \underbrace{\sin^{-1}\left(\frac{x_a}{R_o}\cos\theta_a\right)}_{\text{const 4}}
\end{aligned}
\tag{16}
$$

$$y_f = x_f \left[\cos\left(\frac{\phi_f}{180\pi}\right) \right] \tag{17}$$

Where:

ϕ_f = Angle between χ_a and χ_f

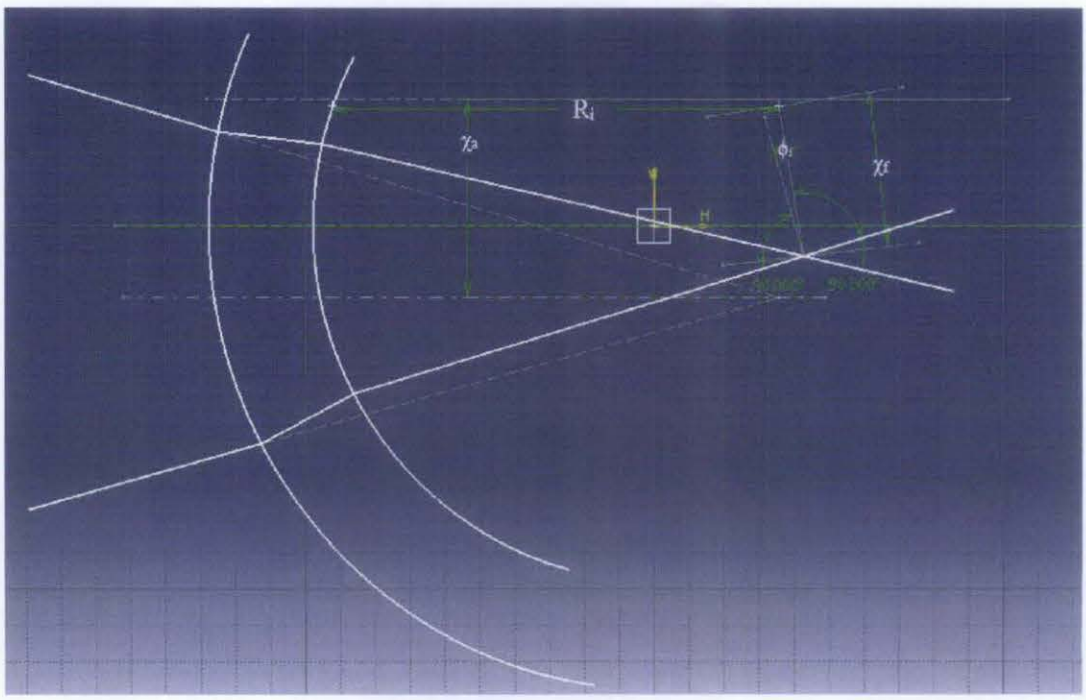

Figure 2.4.4: Refraction of laser beam during radial velocity measurement

All of the above equations require very long calculation due to the correction of refraction that occurs during the LDA measurement upon the cylindrical pipe. The corrections are necessary for the measurement of the three velocity arrangement. Because of this long mathematical derivation, new design for the pipe section is made to reduce the calculation needed for measurement of the refraction correction for fluid velocity. Optical box outside of the pipe and a small cross slit is made on the pipe wall to reduce the mathematical correction for refraction. Only simple positional correction by Bicen is required for all three velocity component measurements.

2.5 Experimental parts and materials

2.5.1 Cylindrical pipe

Material used to make the cylindrical pipe is acrylic. Acrylic is a useful, clear plastic that resembles glass, but has properties that make it better than glass in many ways. Acrylic has been chosen to make various products because of many reasons. One of it is that acrylic is many times stronger than glass, making it much more impact resistant and therefore safer. Acrylic also lighter and insulates better than glass. It also has a transparency rate of 93% makes acrylic the clearest material known. Very thick glass will have a green tint, while acrylic remains clear. Because of this reasons, acrylic have been chosen as the material to make the pipe.

2.5.2 Teflon

Teflon is a synthetic fluoropolymer of tetrafluoroethylene, also known as polytetrafluoroethylene, or PTFE. The molecular structure of Teflon is based on a chain of carbon atoms, the same as all polymers. Unlike some other fluoropolymers, in Teflon this chain is completely surrounded by fluorine atoms. The bond between carbon and fluorine is very strong, and the fluorine atoms shield the vulnerable carbon chain. This unusual structure gives Teflon its unique properties. In addition to its extreme slipperiness, it is inert to almost every known chemical. Normal Teflon has refractive index around 1.35 to 1.38.

PTFE is used as a non-stick coating because of its non-reactivity. It also used in pipework for reactive and corrosive chemicals. PTFE also act as a lubricant since it reduces friction, wear, and energy consumption of machinery. Nowadays, there are many types of Teflon in market.

Teflon PFA film

Teflon PFA film is a thermoplastic film that can be heat sealed, heat bonded, welded, laminated, and used as an excellent hot-melt adhesive. This wide variety of fabrication possibilities combines with important properties to offer a unique balance of capabilities not available in any other plastic film. Specifications of Teflon PFA film is shown in the Appendix.

Teflon FEP film

Teflon FEP film is a transparent, thermoplastic film that can be heat sealed, thermoformed, vacuum formed, heat bonded, welded, metalized, laminated-combined with dozens of other materials, and can also be used as an excellent hot-melt adhesive.

This wide variety of fabrication possibilities combines with important properties to offer a unique balance of capabilities which are not available in any other plastic film. It has higher mechanical strength and optimized for applications in which such light transmission or transparency is required. Therefore, it's also known as transparent Teflon. Specifications of Teflon FEP film is shown in the Appendix.

Based on properties of both Teflons in appendices, it is better to use Teflon FEP since it has lower refractive index than Teflon PFA, which is 1.341.

2.5.3 Gear

Worm gear is used in this setup as it is applicable for slow motion process. For each complete turn of the worm shaft the gear shaft advances only one tooth of the gear and this will reduce the speed of the gear. As the speed is reduced the power to the drive will increase correspondingly. Worm gears are compact and efficient means of substantially decreasing speed and increasing power and it is ideal for use with small electric motors. In this experiment, the worm shaft is rotated using hand and the worm gear will rotate the pipe. For this Test module, Worm gear with size of 50mm of diameter and gear teeth of 70 is used to have gear reduction ratio of 70:1.

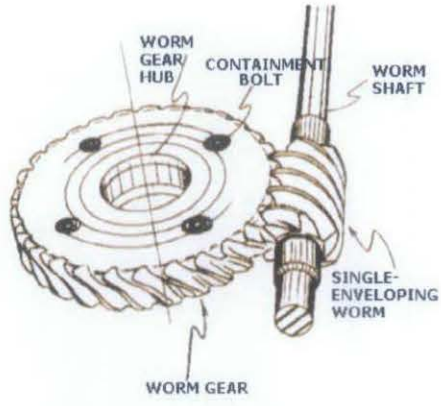

Figure 2.5.3a : Worm gear

2.5.4 Rubber Square Ring (O-Ring)

O-ring is a mechanical gasket in the shape of a disk designed to be fitted in a groove and compressed during assembly between two or more parts, creating a seal at the interface. In this experiment, instead of just being a sealant, square ring is also act as a rotating compartment to rotate the pipe without any leaking. This is achieved by designing a mechanical device that use this square ring to rotate the pipe. Two square rings are placed inside the pipe, one at the rotating pipe and another one at the static pipe.

Figure 2.5.4a : Square Ring

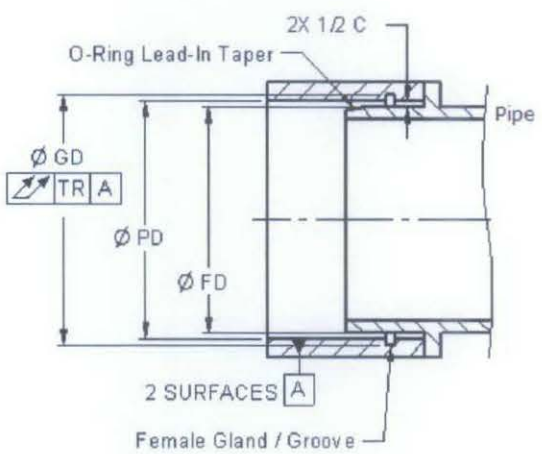

Figure 2.5.4b : Cross section of Square Ring

$$GD\ max = FD\ min + 2L\ max \quad (18)$$

or

$$2L\ max = GD\ min - PD\ min \quad (19)$$

GD = Gland Diameter
PD = Pipe Diameter (adjacent to gland)
FD = Fit Diameter (cylinder which o-ring mates against)

CHAPTER 3
METHODOLOGY

3.1 Procedure Identification

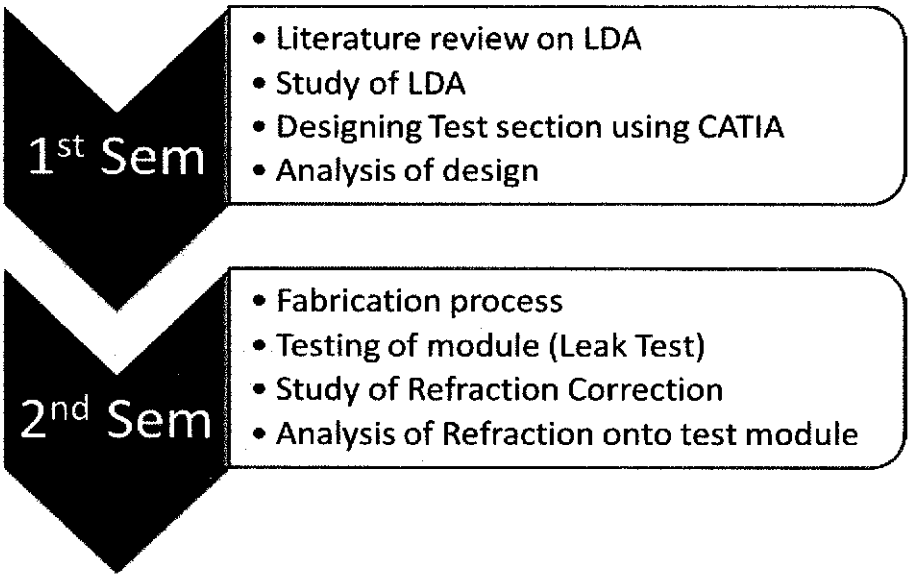

Figure 3.1: Process flow chat

The first step in this project focuses more on the working principle of a Laser Doppler anemometer (LDA). It is also essential to understand the proper steps taken to measure the fluid flow velocity and variables involved in the measurements utilizing LDA. The process parameters such as Reynolds number, friction and head loss also need to be considered when performing the experiments.

Teflon film is integrated in the design of the test section module of the optical box. A suitable type of Teflon film to be utilized in the setup is required in order for the measurements across the optical box to be reliable.

The design of the test section is conducted and assisted by CATIA V5 prior to fabrication. There are many things that need to be taken into consideration in designing the module such as the connection between the optical box and the test section, the test section and the pipe section, and also the module must be rotatable; which can be achieved by placing the gears at the pipe. The designing process takes a very long time because it is very hard to construct the connection parts between the pipes, as leaking still occurred when the test section is rotated.

In second semester, the test section that has been fabricated is tested for leaking between the module and the pipe section. Experiment of the fluid flow in a circular pipe flow loop incorporating the optical box is also to be performed during second semester. The data measured, such as the mean velocity, axial and radial rms velocities will then be compared with those without the optical box to validate this new experimental set-up.

3.2 LDA Systems

To study the characteristics of fluid inside the pipe, Laser Doppler Anemometry (LDA) is used in order to measure mean velocity of the fluid that are flowing inside the pipe. In this experiment, the LDA that will be used is manufactured by Dantec Dynamics that consists of following components which are:

(a) A 300mW argon-ion laser source, LaserPhysics Reliant 500m;

(b) A laser splitter and manipulator, Dantec 60 × 26;

(c) A signal processor, Dantec 58N80-MultiPDA;

(d) Optical-fiber cables, to convey the beams to the transmitter;

(e) A transmitter with a convergent lens, $f = 600$ mm;

(f) A receiver with a convergent lens, $f = 300$ mm;

(g) A traverse system Dantec 57G15; and

(h) Operating software, Sizeware 2.3, installed into a desktop computer.

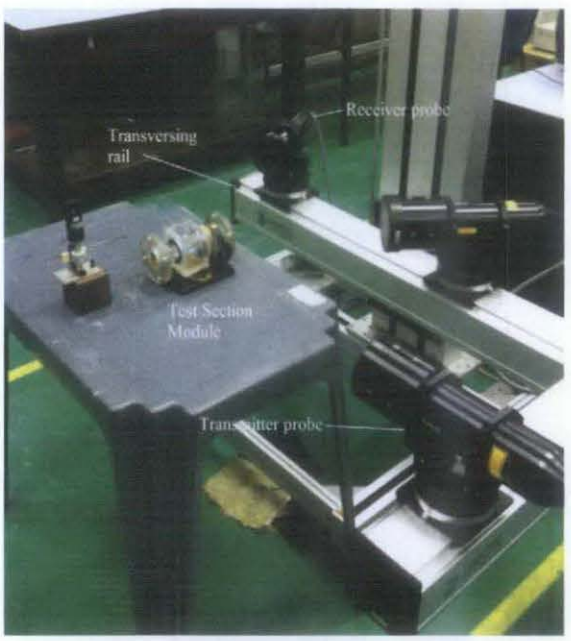

Figure 3.2: Arrangement of the LDA Systems

Shown in the Figure 3.2 is the arrangement of the LDA systems. It consists of two transmitter probes. The first probe is to measure the 2d measurement and the second probe is to measure the 3d measurement. For this project, only the probe for 2d measurement is going to be used. The probe has two pairs of laser which are two vertical and two horizontal laser beams. This pairs of lasers will intersect against each other at a certain distance. The probe can be adjusted horizontally by using the transversing rail. Vertical and horizontal beams will intersect inside the pipe in order to measure fluid velocity.

CHAPTER 4
DISCUSSION

This section will discuss about the design of the test section module. There are two design proposals that have been made for the setup. The designs made were only on the rough surfaces and modification is done later. The hardest part to design is the connection part to connect between the fix pipe and the rotating pipe. The details of each proposal will be discussed on the next section.

The purpose of having the pipe rotatable is to make a measurement at different point using LDA. The pipe is to be rotated 360°, where the slit is rotated around the pipe axis. The main problem addressed here is that leaking will occur at the pipe connection when it is rotated. The only solution to prevent leaking from occuring is by using O-ring where it is a mechanical gasket designed to be placed in a groove and compressed during assembly between two or more parts, creating a seal at the interface. The designs must match with the O-ring structure in order to proceed to fabrication process.

4.1 Design process

4.1.1 1st proposal

For the first proposal, the clamping part will be made by using two solid cylinder rings with a rib on it. One of it will be fixed at the pipe section and the other one will be fixed at the rotating pipe. Rubber will be placed beside the optical box to make sure no leaking occur within the box. The pipe will be rotated using a worm gear, which is placed at the outer pipe wall. The problem with this design is that there will be a large friction between the two rotating cylinder, as the pipe rotate without any lubricant used on the beam. There also will be friction as the pipe flow from one pipe to the other which is not on a smooth surfaces, can cause head loss to the fluid flow inside the pipe. Another problem that may appear is leaking of the fluid as it flows between the two pipes section. O-ring is necessary

in order to prevent leaking from occur, but it is impossible to place the O-ring at the rotating pipe.

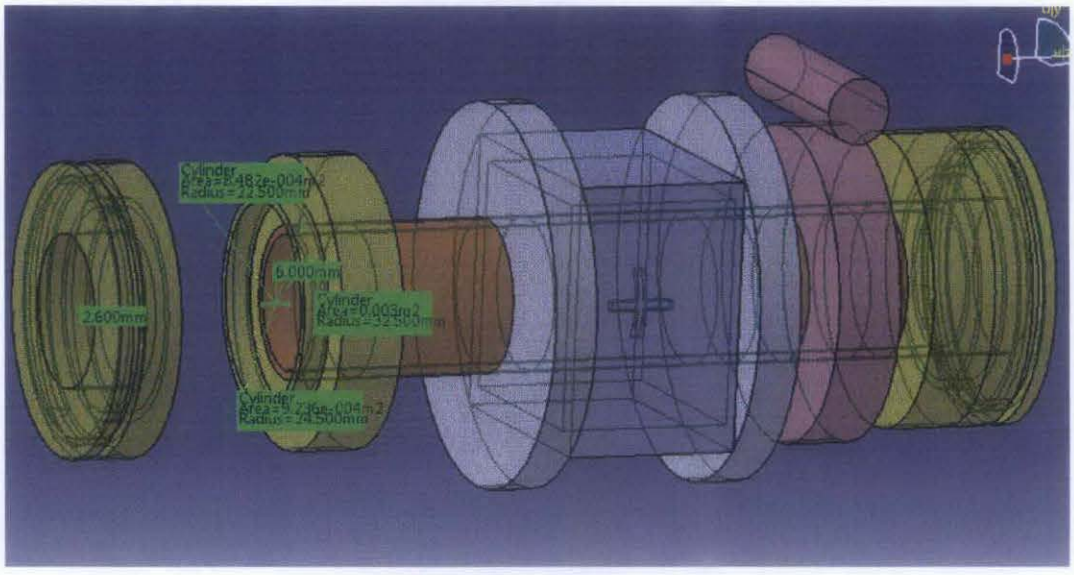

Figure 4.1.1a: 3D view of 1st proposal pipe section

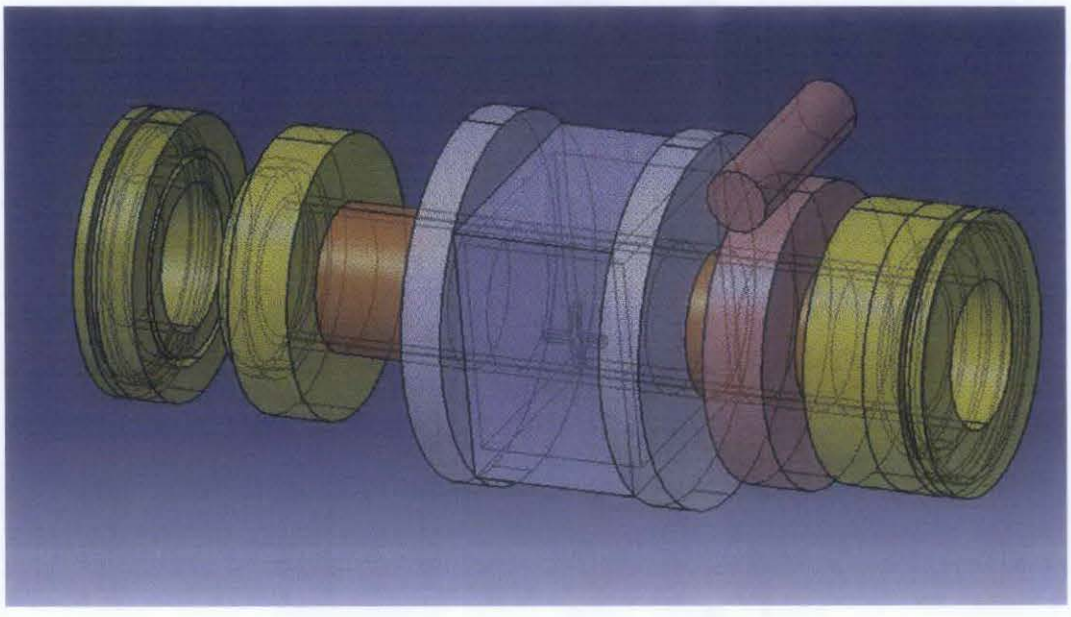

Figure 4.1.1b: 3D view of 1st proposal pipe section

4.1.2 2nd proposal

For the second proposal, the connection to be made between the module and the test section is by using bearing with a mounting. The optical box will be rotated using worm gear, which is placed at the outer pipe wall. The bearing will also be placed at the outer pipe wall, where its inner diameter is same with the outer diameter of the pipe. Mounting is made and fixed to the outer pipe wall at the test section. Bearing will be placed inside the mounting while the two pipes are attached together. This design cause leaking between the connection of the two pipes.

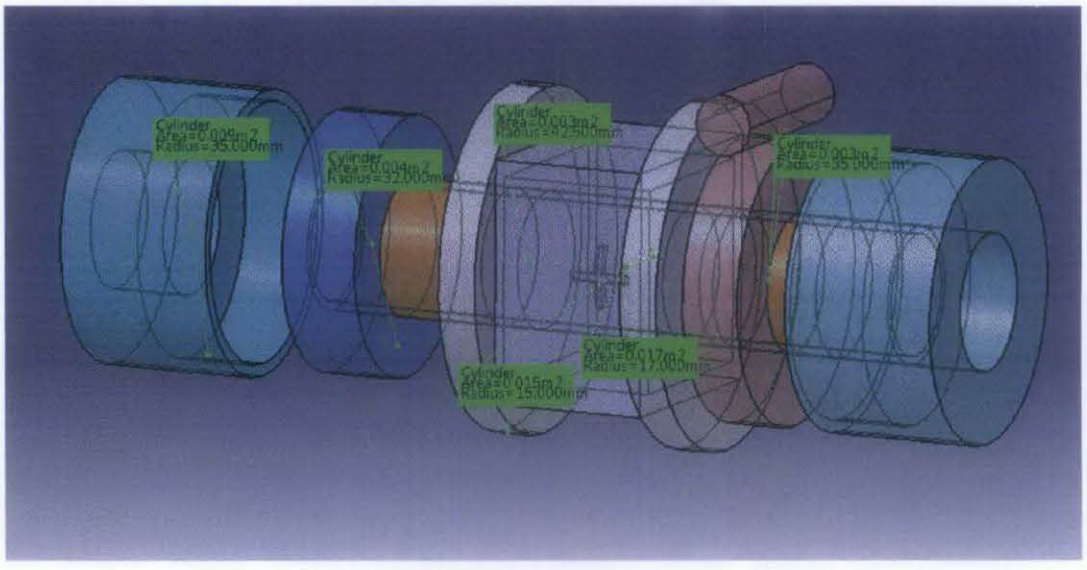

Figure 4.1.2a: 3D view of 2nd proposal pipe section

4.1.3 Design Analysis

To determine the best solution from the two designs, decision matrix is formed in order to compare the two designs based on the selected criteria.

		Design 1		Design 2	
Criteria	Weight	Rating	Score	Rating	Score
Efficiency	40	6	240	8	320
Cost Saving	25	8	200	7	175
Durability	25	6	150	6	150
Appearance	10	6	60	6	60
TOTAL SCORE	~	~	650	~	705

Rating Scale (R)	
Excellent	9 to 10
Good	7 to 8
Fair	5 to 6
Poor	3 to 4
Unsatisfactory	1 to 2

From the result, it can be seen that the proposal of 2nd design is better than the 1st design. Further modification is made upon the 2nd design to include the O-ring into the connection of the pipes to prevent leaking. By adapting the concept of the 2nd design proposal, flange with rubber square ring is used instead of using mounting device to rotate the pipe. Fabrication is made after designing process is completed.

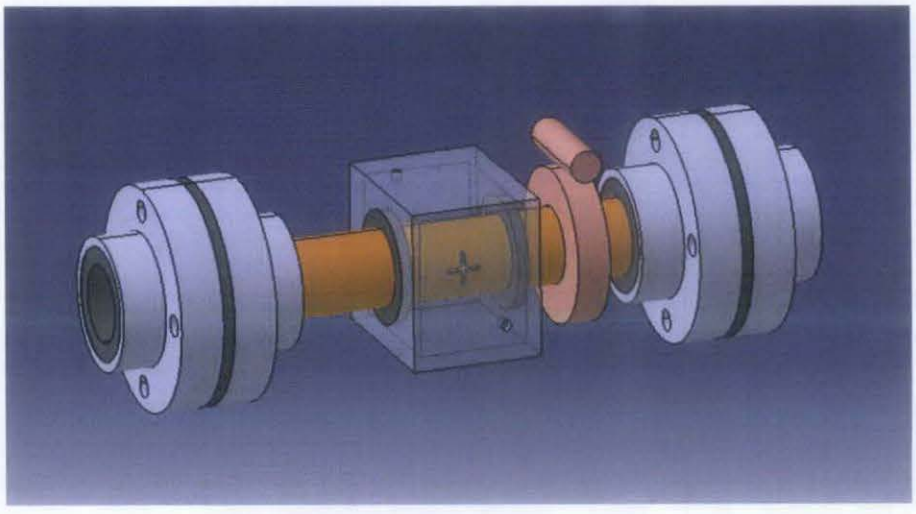

Figure 4.1.3a : 3D view of modified design (based on second proposal)

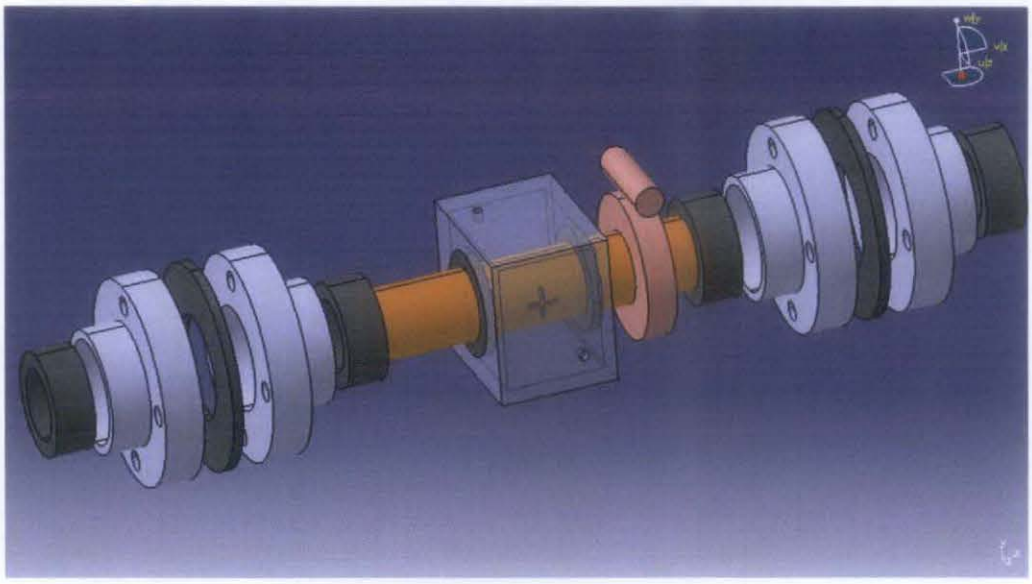

Figure 4.1.3b: Exploded view of modified design (based on second proposal)

4.2 The Test Section

The test section has been fabricated based on the drawing of the second (2^{nd}) proposal with modification made upon the design. The test section is then assembled together with the pipe section and experiment of leak test has been run for three times to make sure there is no leaking at the test section. Below are the actual pictures of the test section.

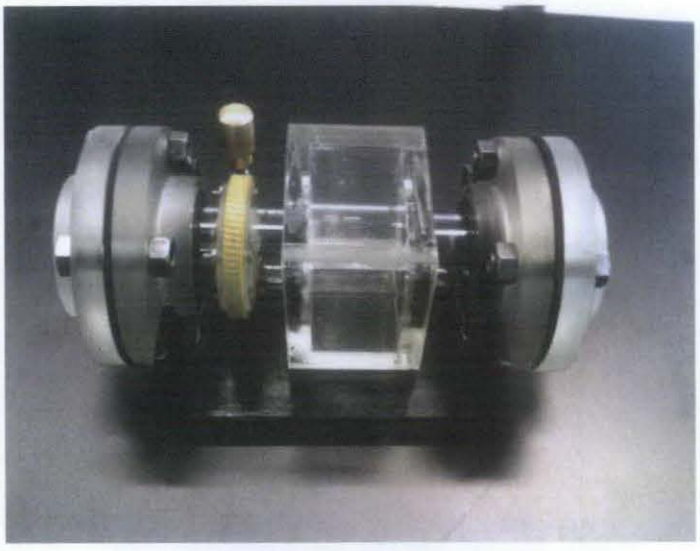

Figure 4.2a: Upper view of Test section

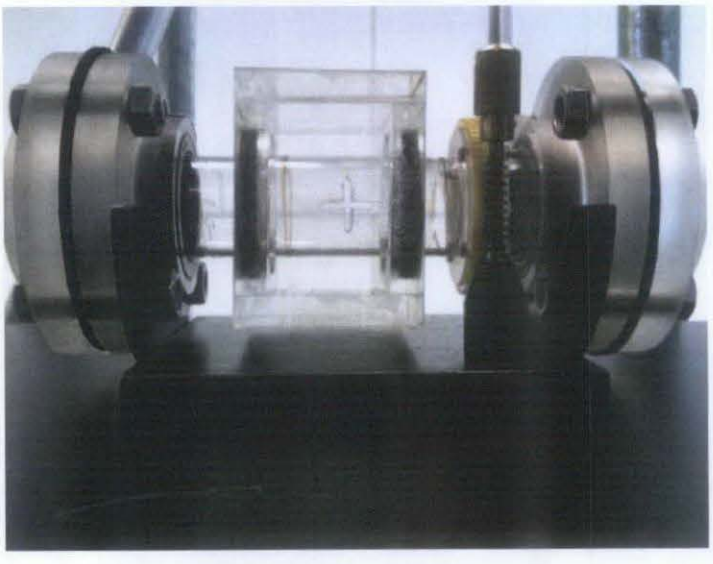

Figure 4.2b: Front view of Test section

Figure 4.2c: Side view of Test section

Figure 4.2d: Perspective view of Test section

There is no leaking occurred at the test section and the design is considered as a success. Experiments using LDA will be conducted using this test section and the result obtained will determine whether this design is useful for future use to reduce refraction at cylindrical surface in order to obtain velocity measurement at axial, tangential and radial components. For the time being, theoretical study is conducted to determine whether this design fulfill the requirement objectives to simplify mathematical derivation for refraction correction.

4.3 Axial (*u'*), Tangential (*w'*), and Radial (*v'*) velocity measurement.

Refraction correction for measurement with and without Teflon film is the same using Bicen's method. To justify the position correction using optical box and without optical box, example of calculation have been conducted.

Example of Calculations For Position Correction.

Parameters:

$n_1 = n_{air} = 1$ (refractive index of air)

$n_2 = n_w = 1.49$ (refractive index of acrylic)

$n_3 = n_f = 1.33$ (refractive index of water)

$t = 2.5$mm (wall thickness)

$R_o = 17.5$ (outer radius of pipe)

$R_i = 15$ (inner radius of pipe)

$x_a = 5$ (assumed)

Assume initial angle of laser beam path is 15°

With Optical box and a cross slit:

Because in this experiment we only consider refraction of laser beam during axial velocity measurement, it is necessary to prove that refraction can be reduced when using the optical box.

Refraction at the optical box: $\boxed{\frac{\sin\theta_1}{\sin\theta_2} = \frac{v_1}{v_2} = \frac{n_2}{n_1}}$

$$\theta_2 = \sin^{-1}\left(\frac{n_1}{n_2}\sin\theta_1\right) = \sin^{-1}\left(\frac{1}{1.49}\sin 15^o\right) = 10^o$$

$$\theta_3 = \sin^{-1}\left(\frac{n_2}{n_3}\sin\theta_2\right) = \sin^{-1}\left(\frac{1.49}{1.33}\sin 10^o\right) = 11.2^o$$

Position of intersection point: $\boxed{x_f = n_f x_a + \underbrace{\left(1-\frac{n_f}{n_w}\right)}_{\text{const 1}} t + \underbrace{(n_f - 1)R_o}_{\text{const 2}}}$

Constant 1: $\left(1-\frac{n_f}{n_w}\right)t = \left(1-\frac{1.33}{1.49}\right)2.5 = 0.2685$

Constant 2: $(n_f - 1)R_o = (1.33-1)17.5 = 5.775$

We must do some correction at the position of intersection point because it may not be in line with the center of the pipe. (See figure 4.3.2)

$$x_f = n_f(x_a + x_{a'}) + \left(1 - \frac{n_f}{n_w}\right)t + (n_f - 1)R_o$$

$$x_{a'} = \frac{\left(1 - \frac{n_f}{n_w}\right)t + (n_f - 1)R_o}{n_f}$$

Or

$$x_f = \left[n_f x_a + \left(1 - \frac{n_f}{n_w}\right)t + (n_f - 1)R_o\right] - x_{f'}$$

$$x_{f'} = \left(1 - \frac{n_f}{n_w}\right)t + (n_f - 1)R_o$$

$$x_f = \left[n_f x_a + \left(1 - \frac{n_f}{n_w}\right)t + (n_f - 1)R_o\right] - x_{f'}$$

$$x_f = [1.33 \times 5 + 0.2685 + 5.775] - (0.2685 + 5.775) = 6.65$$

Distance between virtual intersection point and true intersection point:

$$\Delta x = x_f - x_a = 6.65 - 5 = 1.65$$

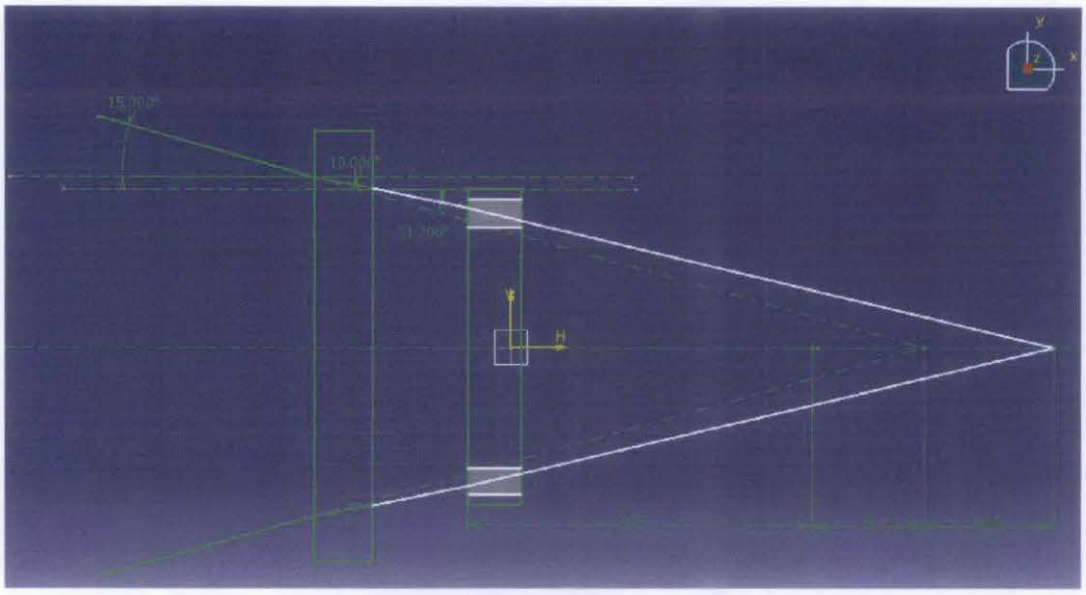

Figure 4.3.1: Refraction of laser beam at axial component
(with optical box)

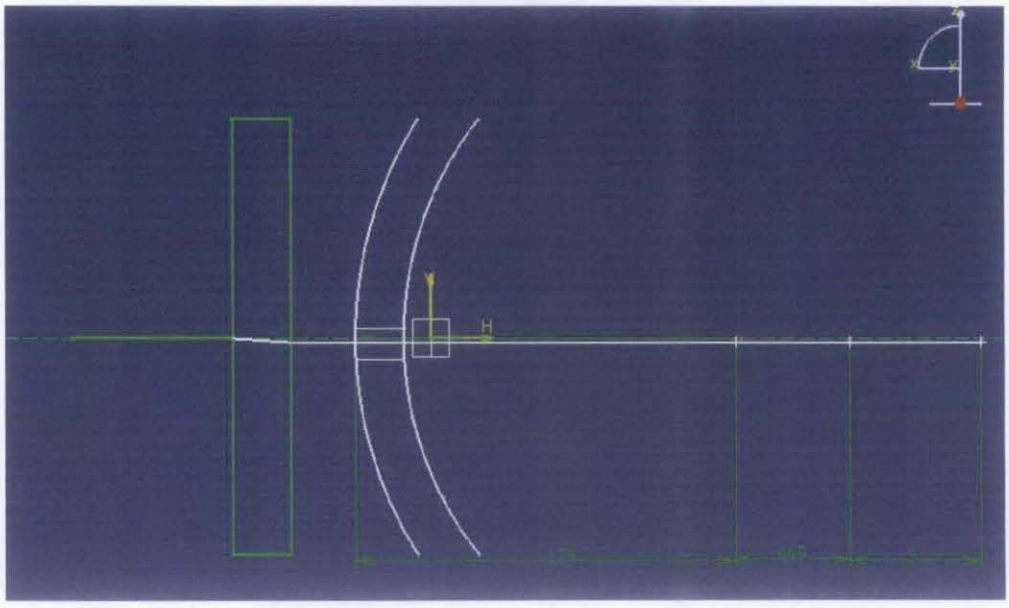

Figure 4.3.2: Refraction of laser beam at axial component from other view
(with optical box)

It can be seen that distance between true point of intersection with refraction and virtual point of intersection without refraction is small, meaning that the intersection point can be easily obtain in the experiment as refraction is reduced.

When using the test section module with an optical box, laser beam will propagate to the optical box and it will be refracted nearer to its normal line. As the beam goes through the pipe curvature, it will enter the cross slit section and will not refracted. Refraction only occurs at axial position at the flat surface of the optical box as the laser beam goes through the flat surface of the optical box. This will eliminate any correction for refraction that is necessary for the cylindrical curvature at tangential and radial components.

Without Optical box and cross slit:

Axial component:

$$x_f = n_f x_a + \underbrace{\left(1 - \frac{n_f}{n_w}\right)}_{\text{const 1}} t + \underbrace{(n_f - 1)R_o}_{\text{const 2}}$$

$x_a = -5$

Constant 1: $\left(1 - \frac{n_f}{n_w}\right)t = \left(1 - \frac{1.33}{1.49}\right)2.5 = 0.2685$

Constant 2: $(n_f - 1)R_o = (1.33 - 1)17.5 = 5.775$

$$x_f = \left[n_f x_a + \left(1 - \frac{n_f}{n_w}\right)t + (n_f - 1)R_o\right] - x_{f'}$$

$$x_f = [1.33 \times -5 + 0.2685 + 5.775] - (0.2685 + 5.775) = -6.65$$

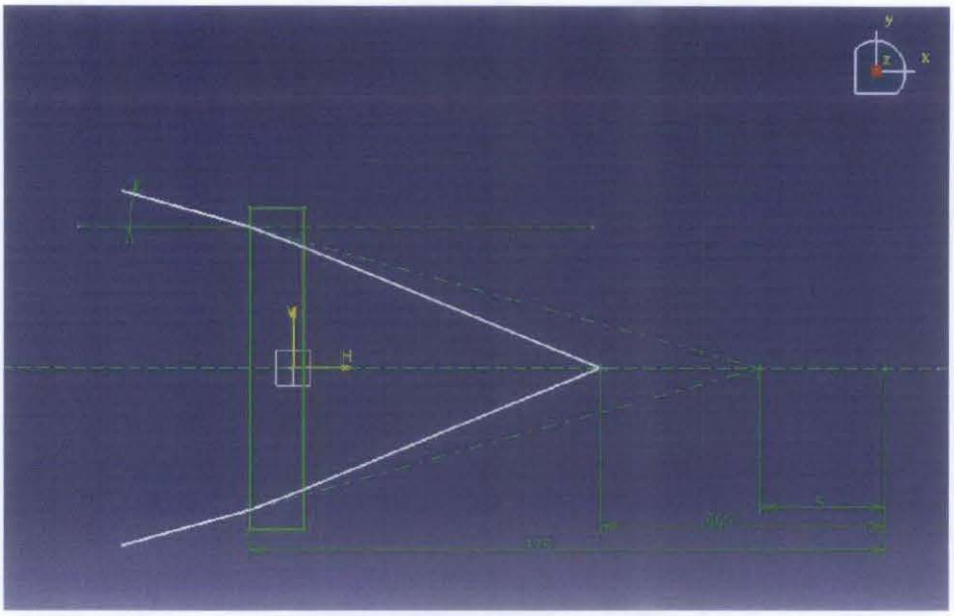

Figure 4.3.3: Refraction of laser beam at axial component

(without optical box)

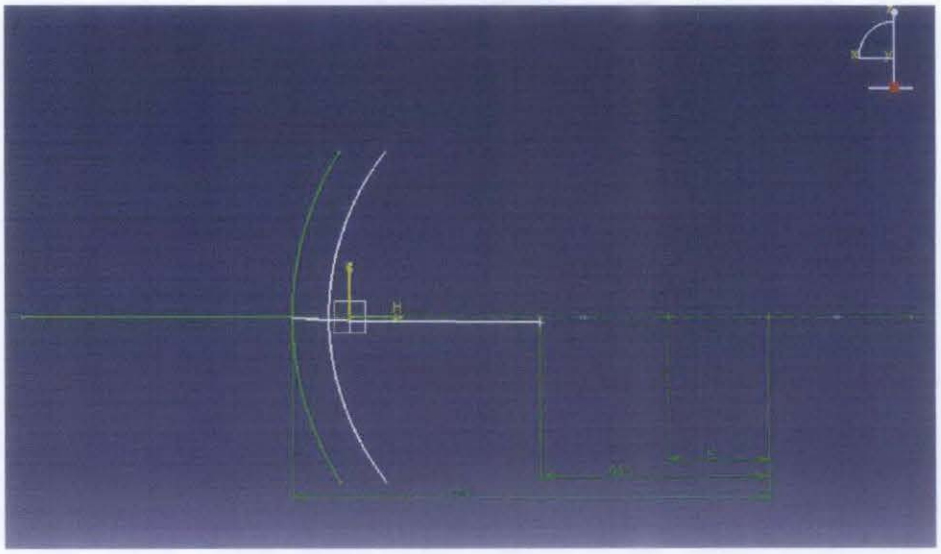

Figure 4.3.4: Refraction of laser beam at axial component from other view

(without optical box)

Tangential component:

$$C_f = \frac{1}{\underbrace{n_f}_{\text{const 1}}} \frac{1}{\left[1+\left(\frac{r_a}{R_o}\right)\left[\underbrace{\left(\frac{R_o}{R_i}\right)\frac{\left(\frac{n_f}{n_w}-1\right)}{n_f}}_{\text{const 2}} + \underbrace{\frac{n_w-1}{n_w}}_{\text{const 3}}\right]\right]}$$

$$x_f = C_f x_a$$

$$V_f = C_f V_a$$

Constant 1: $n_f = 1.33$

Constant 2: $\left(\frac{R_o}{R_i}\right)\frac{\left(\frac{n_f}{n_w}-1\right)}{n_f} = \left(\frac{17.5}{15}\right)\frac{\left(\frac{1.33}{1.49}-1\right)}{1.33} = -0.0942$

Constant 3: $\frac{n_w-1}{n_w} = \frac{1.49-1}{1.49} = 0.3289$

$$C_f = \frac{1}{1.33}\frac{1}{\left[1+\left(\frac{5}{17.5}\right)\left[-0.0942+0.3289\right]\right]} = 0.705$$

$$x_f = C_f x_a = 0.705 \times 5 = 3.52$$

For tangential position, need to add up the true point of intersection with inner radius.

$$x_f = 3.52 + 15 = 18.52$$

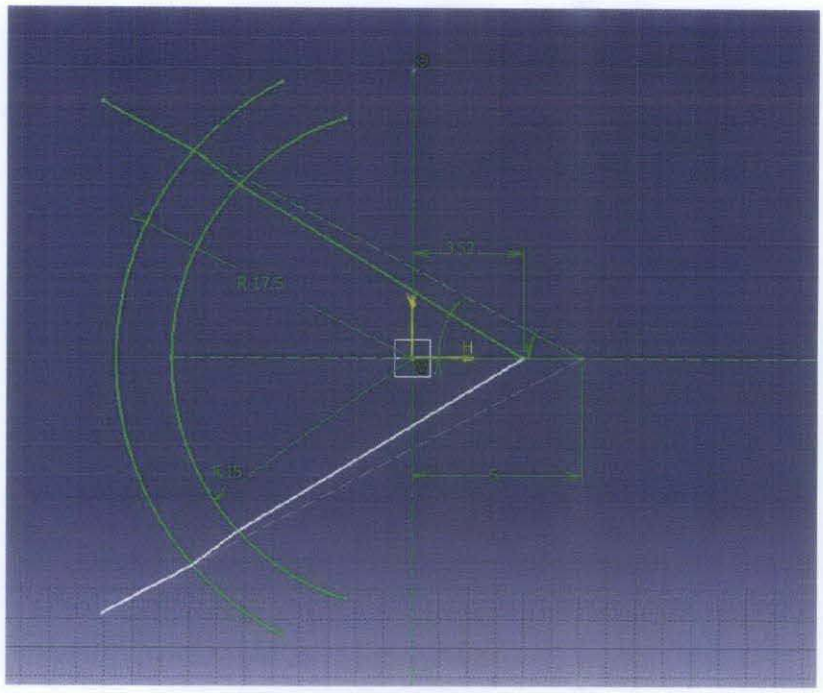

Figure 4.3.5: Refraction of laser beam at tangential component (without optical box)

Radial component:

$$C_f = \frac{1}{n_f}$$

$$x_f = C_f x_a$$

$$V_f = C_f V_a$$

$$\phi_f = \underbrace{\sin^{-1}\left(\frac{x_a}{n_w R_i}\cos\theta_a\right)}_{\text{const 1}} \underbrace{-\sin^{-1}\left(\frac{x_a}{n_w R_o}\cos\theta_a\right)}_{\text{const 2}}$$

$$\underbrace{-\sin^{-1}\left(\frac{x_a}{n_f R_i}\cos\theta_a\right)}_{\text{const 3}} + \underbrace{\sin^{-1}\left(\frac{x_a}{R_o}\cos\theta_a\right)}_{\text{const 4}}$$

$$C_f = \frac{1}{n_f} = \frac{1}{1.33} = 0.7518$$

$$x_f = C_f x_a = 0.7518 \times 5 = 3.7594$$

Constant 1: $\sin^{-1}\left(\frac{x_a}{n_w R_i}\cos\theta_a\right)=\sin^{-1}\left[\frac{5}{1.49\times 15}\cos 15^o\right]=12.47^o$

Constant 2: $\sin^{-1}\left(\frac{x_a}{n_w R_o}\cos\theta_a\right)=\sin^{-1}\left[\frac{5}{1.49\times 17.5}\cos 15^o\right]=10.67^o$

Constant 3: $\sin^{-1}\left(\frac{x_a}{n_f R_i}\cos\theta_a\right)=\sin^{-1}\left[\frac{5}{1.33\times 15}\cos 15^o\right]=14.01^o$

Constant 4: $\sin^{-1}\left(\frac{x_a}{R_o}\cos\theta_a\right)=\sin^{-1}\left[\frac{5}{17.5}\cos 15^o\right]=16.02^o$

$\phi_f = 12.47-10.67-14.01+16.02=3.81^o$

$y_f = x_f\left[\cos(\frac{\phi_f}{180\pi})\right]$

$y_f = 3.7594\left[\cos(\frac{3.81^o}{180\pi})\right]=3.75$

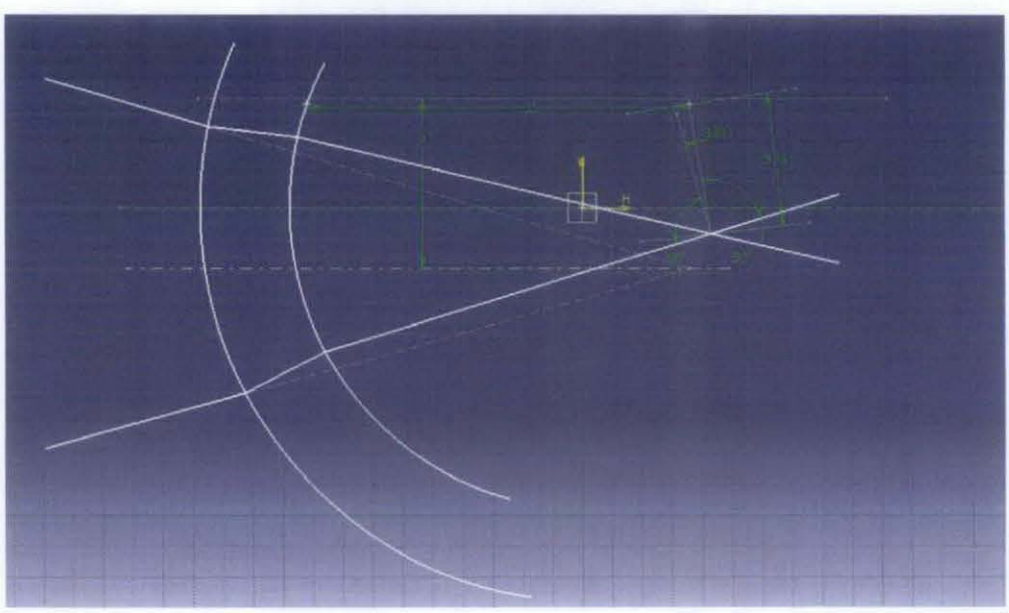

Figure 4.3.6: Refraction of laser beam at radial component (without optical box)

When using cylindrical pipe without the optical box and cross slit, refraction that occur is very severe at the curvature surface. Laser beam is refracted further away from normal line at tangential and radial position. At axial position, the true point of intersection lies in front of the cylindrical pipe center point, because the surface curvature of the pipe focuses the laser beam near the pipe wall. The beam angle is not important here since the only thing that needs to be considered is the distance of the virtual position of intersection without refraction. The value of axial position between refraction with optical box and without the optical box might be the same as the curvature does not affect the position of axial component significantly. The major things that will be affected when not using the optical box are the position at tangential and radial components. The distance between true point of intersection and virtual point of intersection without refraction increases at radial and tangential positions making it hard to obtain the intersection point when conducting the experiments.

It can be seen that the mathematical derivation for refraction correction when using optical box and cross slit module is much simpler compared to cylindrical pipe without the optical box and the cross slit. Refraction is reduced when using optical box and cross slit module as the distance between virtual intersection point and true intersection point is reduced and the tangential and radial component are neglected.

CHAPTER 5
CONCLUSION

For the time being, the experiment analysis using LDA to test the test section module cannot be conducted due to the unavailability of the equipment. The design of the test section module is conducted in details in order to prevent any error occur during experiments. Leak test that has been conducted upon the test section prove that the design is done successfully. Theoretical study shows a positive result of the ability of the optical box to reduce laser beam refraction, thus simplify mathematical derivation of refraction correction.

The designed optical box is expected to utilize the measurement for very near pipe wall and simplifies the mathematical derivation based on refraction of the laser beam. This optical box is constructed outside the pipe and a small cross slit module is made at the pipe wall for laser beam to pass through it and to reduce refraction. The pipe is rotatable using worm gear in order to take measurement at different points and compare it with each other. With reference from previous experiments conducted, this project ought to be a great solution to measure fluid flow velocity near pipe wall with a little mathematical derivations involved.

REFERENCES

1. Drain, L.E., 1980, *The Laser Doppler Technique*, John Wiley & Sons Ltd.

2. E. Durst, A. Melling and L.H. Whitelaw, 1981, *Principles and Practice of Laser Doppler Anemometry*, University of Karlsruhe, West Germany, Brown, Boveri and Co. Ltd, Switzerland, Imperial College of Science and Technology, England.

3. D. Poggi, A. Porporato, L. Ridolfi, *An experimental contribution to near-wall measurements by means of a special laser Doppler anemometry technique.*

4. J. M. J. den Toonder, F. T. M. Nieuwstadt, 1997, *Reynolds number effects in a turbulent pipe flow for low to moderate Re,* Laboratory Aero and Hydrodynamics, Delft University of Technology, Retterdamseweg 145, The Netherlands.

5. A.F. Bicen, 1982, *Refraction Correction for LDA Measurement In Flows Wish Curved Optical Boundaries,* Imperial College of Science and Technology, England.

6. John D. Boadway and Emin Karahan, 1981, *Correction of Laser Doppler Anemometer Readings for Refraction at Cylindrical Interface,* Queen's University, Canada, Istanbul Teknik Universitesi, Turkey.

7. A. Japper-Jaafar, M.P. Escudier, R.J. Poole, 2009, *Journal of Non-Newtonian Fluid Mechanics,* Department of Engineering, University of Liverpool, United Kingdom.

8. M.P. Escudier, I.W. Gouldson, A.S. Pereira, F.T. Pinho, R.J. Poole, 2001, *Non-Newtonian Fluid Mechanics,* University of Liverpool, United Kingdom.

9. C Tropea, 1995, *Laser Doppler anemometry: recent developments and future challenges,* Meas. Sci. Technol.

10. Wikipedia, 2009, *Laser Doppler Anemometry*, <http://en.wikipedia.org/wiki/Laser_Doppler_velocimetry >

11. Wikipedia, 2009, *Worm gear*, < http://en.wikipedia.org/wiki/Worm_drive >

12. DuPont, 2009, *Teflon film*, <http://www2.dupont.com/Teflon_Industrial/en_US/products/product_by_name/index.html>

13. Marco, 2009, *Square ring*, < http://www.marcorubber.com/square_rings.htm >

14. Wikipedia, 2009, *Acrylic*, < http://en.wikipedia.org/wiki/Acrylic >

APPENDICES

	Property	Test Method	Typical Value*	
			SI Units	English Units
Mechanical	Tensile Strength at Break	ASTM D-882	21 N/mm²	3000 psi
	Elongation at Break	ASTM D-882	300%	
	Yield Point	ASTM D-882	12 MPa	1700 psi
	Elastic Modulus	ASTM D-882	480 MPa	70,000 psi
	Impact Resistance	DuPont pneumatic impact tester	6.2×10^4	14 in-lb/mil
	Folding Endurance (MIT)	ASTM D-2176	100,000 cycles	
	Tear Strength—Initial (Graves)	ASTM D-1004	4.90 N	500 g
	Tear Strength—Propagating (Elmendorf)	ASTM D-1922	0.74 N	75 g
Thermal	Melt Point	ASTM D-3418 (DTA)	302–310°C	575–590°F
	Thermal Conductivity	Cenco-Fitch	0.195 W/(m·K)	1.35 Btu·in/(h·ft²·°F)
	Specific Heat	—	1172 J/(kg·K)	0.28 Btu/(lb·°F)
	Dimensional Stability	30 min at 150°C (302°F)	MD = 1% shrinkage TD = 1% shrinkage	
	Oxygen Index	ASTM D-2863	95%	
Electrical	Dielectric Strength, short-time, in air at 23°C (73°F), 6.35 mm (¼ in) diameter electrode, 0.79 mm (1/32 in) radius, 60 Hz, 500 V/s rate of rise: 0.025 mm (1 mil) film	ASTM D-149 Method A	260 kV/mm	6500 V/mil
	Dielectric Constant, 25°C (77°F), 100 Hz to 1 MHz	ASTM D-150	2.0	
	Dissipation Factor, 25°C (77°F), 100 Hz to 1 MHz	ASTM D-150	0.0002–0.0007	
	Volume Resistivity, −40 to 240°C (−40 to 464°F)	ASTM D-257	$>1 \times 10^{17}$ ohm·cm	
Chemical	Moisture Absorption	—	<0.02%	
	Permeability, Gas:	ASTM D-1434	cm³/(m² 24 h·atm)**	
	Carbon Dioxide		14×10^3	
	Nitrogen		2.0×10^3	
	Oxygen		6.7×10^3	
	Permeability, Vapors:	ASTM E-96	g/(m²·d)	g/(100 in² 24 h)
	Water		2	0.13
	Teflon® is chemically inert and solvent resistant to virtually all chemicals, except molten alkali metals, gaseous fluorine, and certain complex halogenated compounds, such as chlorine trifluoride at elevated temperatures and pressures.			
Misc.	Density	ASTM D-1505	2150 kg/m³	134 lb/ft³
	Coefficient of Friction Kinetic (Film-to-Steel)	ASTM D-I 894	0.1–0.3	
	Refractive Index	ASTM D-542	1.350	
	Solar Transmission	ASTM E-424	96%	

Table 1: Properties of Teflon PFA film

		Typical Value[a]	
Property	**Test Method**	**SI Units**	**English Units**
Mechanical			
Tensile Strength at Break	ASTM D-882	21 N/mm²	3000 psi
Elongation at Break	ASTM D-882	300%	
Yield Point	ASTM D-882	12 MPa	1700 psi
Elastic Modulus	ASTM D-882	480 MPa	70,000 psi
Impact Strength	DuPont pneumatic impact tester	7.7×10^3 J/m	144 ft-lb/in
Folding Endurance (MIT)	ASTM D-2176	10,000 cycles	
Tear Strength–Initial (Graves)	ASTM D-1004	2.65 N	270 g force
Tear Strength–Propagating (Elmendorf)	ASTM D-1922	1.23 N	125 g
Bursting Strength (Mullen)	ASTM D-774	76 kPa	11 psi
Thermal			
Melt Point	ASTM D-3418 (DTA)	260–280°C	500–536°F
Zero Strength Temperature	b	255°C	490°F
Coefficient of Thermal Conductivity	Cenco-Fitch	0.195 W/m×K	1.35 Btu×in/h×ft²×°F
Specific Heat	—	1172 J/kg×K	0.28 Btu/lb×°F
Heat Deflection Temperature at 0.46 N/mm2 (66 psi) at 1.82 N/mm2 (264 psi)	ASTM D-648 Tensile Bars	 70°C 51°C	 158°F 124°F
Dimensional Stability	30 min at 150°C (302°F)	MD = 0.72% expansion TD = 2.2% shrinkage	
Flammability Classification[c]	ANSI/UL 94	VTM-0	
Oxygen Index	ASTM D-2863	95%	
Miscellaneous			
Density	ASTM D-1505	2150 kg/m³	134 lb/ft³
Coefficient of Friction, Kinetic (Film-to-Steel)	ASTM D-1894	0.1–0.3	
Refractive Index	ASTM D-542	1.341–1.347	
Solar Transmission	ASTM E-424	96%	

Table 2: Properties of Teflon FEP film

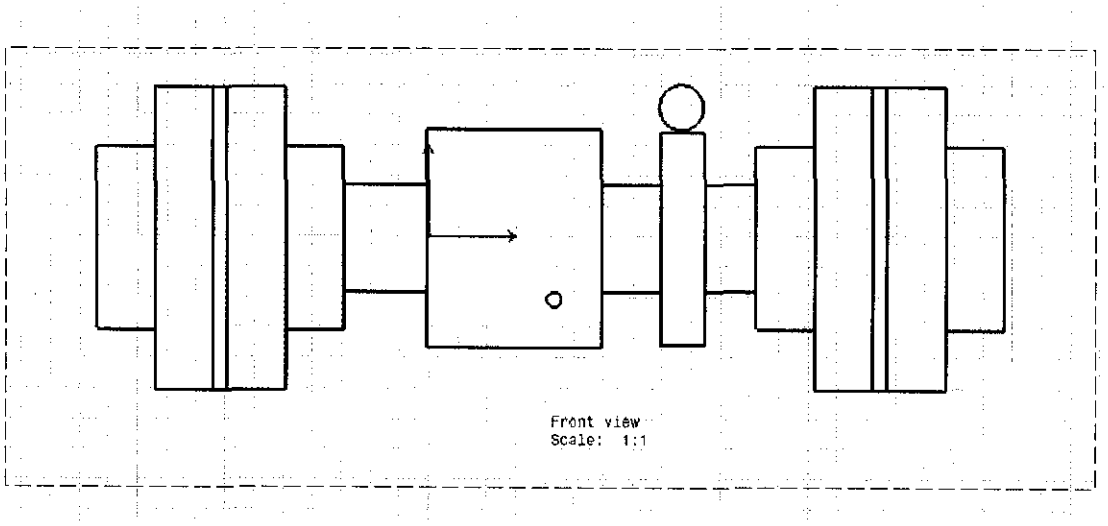

Figure 4.1.3c: Drawing of the Test Section Module

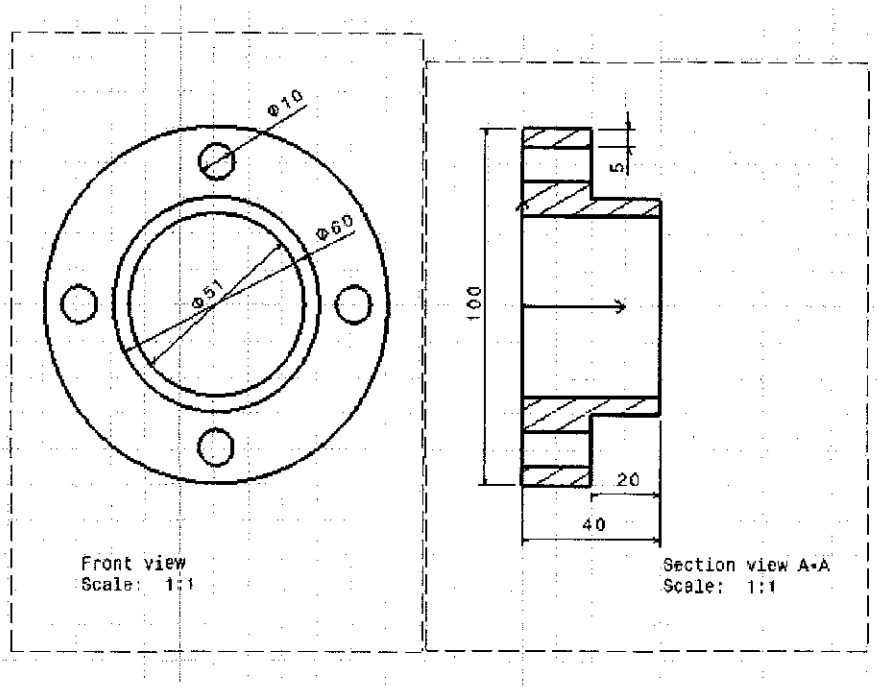

Figure 4.1.3d: Drawing of Flange

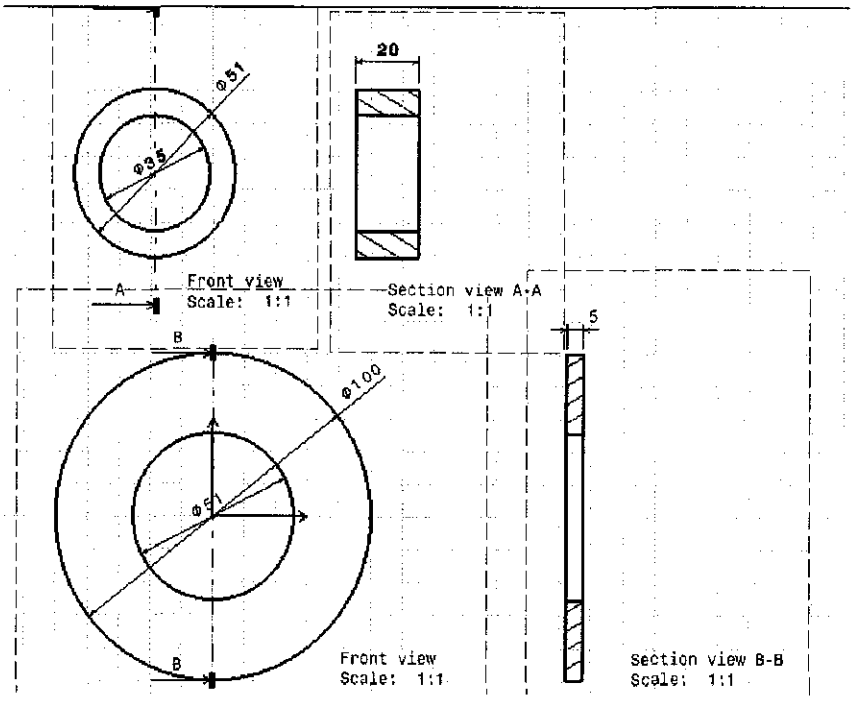

Figure 4.1.3e: Drawings of Square O-Ring and Gasket

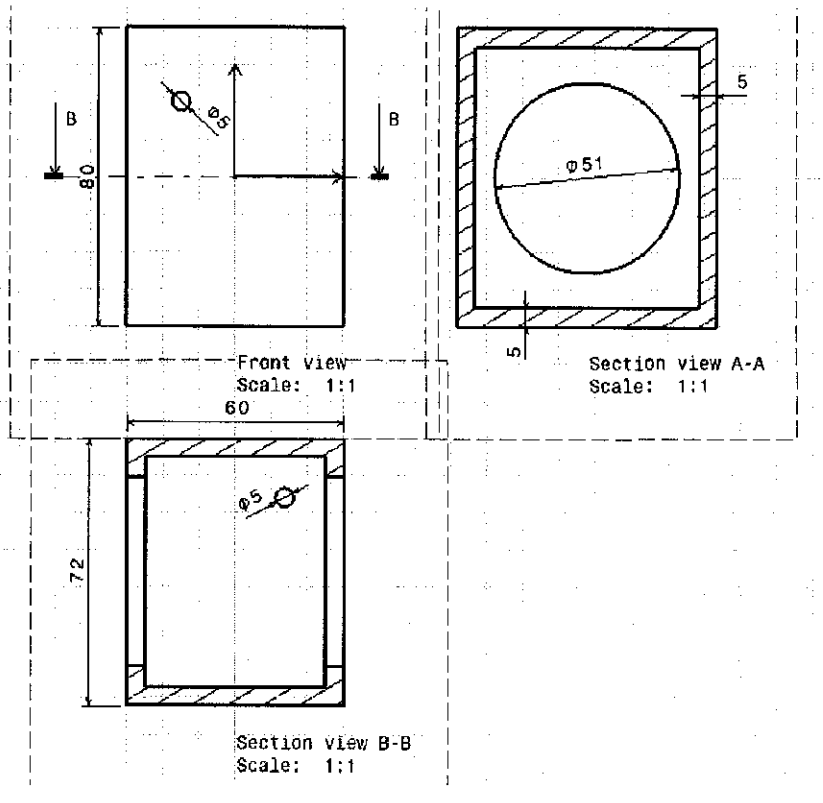

Figure 4.1.3f: Drawing of an Optical box

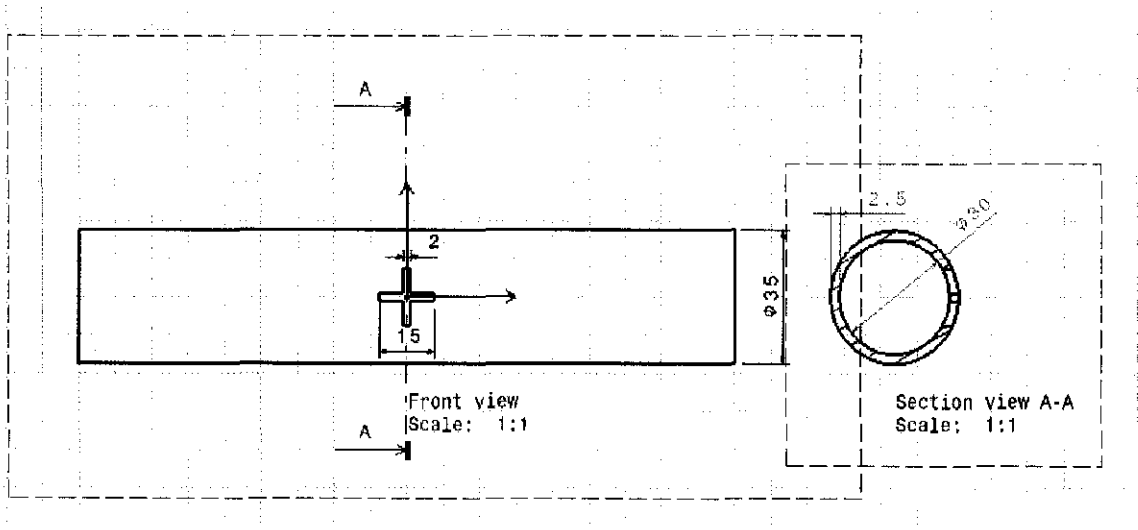

Figure 4.1.3g: Drawing of Pipe with cross slit

Refraction Calculation (Axial Component, Bicen)

*with and without the Optical box and Cross Slit have same result for position correction, except that result with optical box have positive sign (behind pipe center point) and result without optical box have negative sign (in front of pipe center point).

$$x_f = n_f x_a + \underbrace{\left(1 - \frac{n_f}{n_w}\right)}_{\text{const 1}} t + \underbrace{(n_f - 1)R_o}_{\text{const 2}}$$

x_a	x_f	x_f	Wall Thickness (mm)	t
			2.5	
0.00	0.00	0.00		
0.20	0.27	0.27	Fluid RI	n_f
0.40	0.53	0.53	1.33	
0.60	0.80	0.80		
0.80	1.06	1.06	Wall RI	n_w
1.00	1.33	1.33	1.49	
1.20	1.60	1.60		
1.40	1.86	1.86	Inner Radius (mm)	R_i
1.60	2.13	2.13	15	
1.80	2.39	2.39		
2.00	2.66	2.66	Outer Radius (mm)	R_o
2.20	2.93	2.93	17.5	
2.40	3.19	3.19		
2.60	3.46	3.46	Const 1	
2.80	3.72	3.72	0.268456	
3.00	3.99	3.99		
3.20	4.26	4.26	Const 2	
3.40	4.52	4.52	5.775	
3.60	4.79	4.79		
3.80	5.05	5.05	Xa Correction	
4.00	5.32	5.32	-4.54395	
4.20	5.59	5.59		
4.40	5.85	5.85	Xf Correction	
4.60	6.12	6.12	6.043456	
4.80	6.38	6.38		
5.00	6.65	6.65		
5.20	6.92	6.92		
5.40	7.18	7.18		
5.60	7.45	7.45		
5.80	7.71	7.71		
6.00	7.98	7.98		
6.20	8.25	8.25		
6.40	8.51	8.51		
6.60	8.78	8.78		
6.80	9.04	9.04		

7.00	9.31	9.31
7.20	9.58	9.58
7.40	9.84	9.84
7.60	10.11	10.11
7.80	10.37	10.37
8.00	10.64	10.64
8.20	10.91	10.91
8.40	11.17	11.17
8.60	11.44	11.44
8.80	11.70	11.70
9.00	11.97	11.97
9.20	12.24	12.24
9.40	12.50	12.50
9.60	12.77	12.77
9.80	13.03	13.03
10.00	13.30	13.30
10.20	13.57	13.57
10.40	13.83	13.83
10.60	14.10	14.10
10.80	14.36	14.36
11.00	14.63	14.63
11.20	14.90	14.90
11.40	15.16	15.16
11.60	15.43	15.43
11.80	15.69	15.69
12.00	15.96	15.96
12.20	16.23	16.23
12.40	16.49	16.49
12.60	16.76	16.76
12.80	17.02	17.02
13.00	17.29	17.29
13.20	17.56	17.56
13.40	17.82	17.82
13.60	18.09	18.09
13.80	18.35	18.35
14.00	18.62	18.62
14.20	18.89	18.89
14.40	19.15	19.15
14.60	19.42	19.42
14.80	19.68	19.68
15.00	19.95	19.95
15.20	20.22	20.22
15.40	20.48	20.48
15.60	20.75	20.75
15.80	21.01	21.01
16.00	21.28	21.28
16.20	21.55	21.55
26.00	34.58	34.58

16.40	21.81	21.81
16.60	22.08	22.08
16.80	22.34	22.34
17.00	22.61	22.61
17.20	22.88	22.88
17.60	23.41	23.41
17.80	23.67	23.67
18.00	23.94	23.94
18.20	24.21	24.21
18.40	24.47	24.47
18.60	24.74	24.74
18.80	25.00	25.00
19.00	25.27	25.27
19.20	25.54	25.54
19.40	25.80	25.80
19.60	26.07	26.07
19.80	26.33	26.33
20.00	26.60	26.60
20.20	26.87	26.87
20.40	27.13	27.13
20.60	27.40	27.40
20.80	27.66	27.66
21.00	27.93	27.93
21.20	28.20	28.20
21.40	28.46	28.46
21.60	28.73	28.73
21.80	28.99	28.99
22.00	29.26	29.26
22.20	29.53	29.53
22.40	29.79	29.79
22.60	30.06	30.06
22.80	30.32	30.32
23.00	30.59	30.59
23.20	30.86	30.86
23.40	31.12	31.12
23.60	31.39	31.39
23.80	31.65	31.65
24.00	31.92	31.92
24.20	32.19	32.19
24.40	32.45	32.45
24.60	32.72	32.72
24.80	32.98	32.98
25.00	33.25	33.25
25.20	33.52	33.52
25.40	33.78	33.78
25.60	34.05	34.05
25.80	34.31	34.31

26.20	34.85	34.85
26.40	35.11	35.11
26.60	35.38	35.38
26.80	35.64	35.64
27.00	35.91	35.91
27.20	36.18	36.18
27.40	36.44	36.44
27.60	36.71	36.71
27.80	36.97	36.97
28.00	37.24	37.24
28.20	37.51	37.51
28.40	37.77	37.77
28.60	38.04	38.04
28.80	38.30	38.30
29.00	38.57	38.57
29.20	38.84	38.84
29.40	39.10	39.10
29.60	39.37	39.37
29.80	39.63	39.63
30.00	39.90	39.90

Refraction Calculation (Tangential Component, Bicen)

*Without Optical box and cross slit

				From cylinder wall X_a+R_i		From cylinder axi R_f-X_a
x_a	r/R	C_f	x_f	x_a	x_f	x_a
0	0	0.75	0.0000	15.0000	15.0000	15.00
0.20	0.013333333	0.75	0.1500	15.2000	15.1500	14.80
0.40	0.026666667	0.75	0.2991	15.4000	15.2991	14.60
0.60	0.04	0.75	0.4475	15.6000	15.4475	14.40
0.80	0.053333333	0.74	0.5951	15.8000	15.5951	14.20
1.00	0.066666667	0.74	0.7419	16.0000	15.7419	14.00
1.20	0.08	0.74	0.8880	16.2000	15.8880	13.80
1.40	0.093333333	0.74	1.0332	16.4000	16.0332	13.60
1.60	0.106666667	0.74	1.1777	16.6000	16.1777	13.40
1.80	0.12	0.73	1.3215	16.8000	16.3215	13.20
2.00	0.133333333	0.73	1.4645	17.0000	16.4645	13.00
2.20	0.146666667	0.73	1.6067	17.2000	16.6067	12.80
2.40	0.16	0.73	1.7482	17.4000	16.7482	12.60
2.60	0.173333333	0.73	1.8890	17.6000	16.8890	12.40
2.80	0.186666667	0.72	2.0291	17.8000	17.0291	12.20
3.00	0.2	0.72	2.1684	18.0000	17.1684	12.00
3.20	0.213333333	0.72	2.3070	18.2000	17.3070	11.80
3.40	0.226666667	0.72	2.4449	18.4000	17.4449	11.60
3.60	0.24	0.72	2.5821	18.6000	17.5821	11.40
3.80	0.253333333	0.72	2.7186	18.8000	17.7186	11.20
4.00	0.266666667	0.71	2.8544	19.0000	17.8544	11.00
4.20	0.28	0.71	2.9895	19.2000	17.9895	10.80
4.40	0.293333333	0.71	3.1240	19.4000	18.1240	10.60
4.60	0.306666667	0.71	3.2577	19.6000	18.2577	10.40
4.80	0.32	0.71	3.3908	19.8000	18.3908	10.20
5.00	0.333333333	0.70	3.5232	20.0000	18.5232	10.00
5.20	0.346666667	0.70	3.6549	20.2000	18.6549	9.80
5.40	0.36	0.70	3.7860	20.4000	18.7860	9.60
5.60	0.373333333	0.70	3.9164	20.6000	18.9164	9.40
5.80	0.386666667	0.70	4.0462	20.8000	19.0462	9.20
6.00	0.4	0.70	4.1753	21.0000	19.1753	9.00
6.20	0.413333333	0.69	4.3038	21.2000	19.3038	8.80
6.40	0.426666667	0.69	4.4317	21.4000	19.4317	8.60
6.60	0.44	0.69	4.5589	21.6000	19.5589	8.40
6.80	0.453333333	0.69	4.6855	21.8000	19.6855	8.20
7.00	0.466666667	0.69	4.8115	22.0000	19.8115	8.00
7.20	0.48	0.69	4.9369	22.2000	19.9369	7.80
7.40	0.493333333	0.68	5.0616	22.4000	20.0616	7.60
7.60	0.506666667	0.68	5.1858	22.6000	20.1858	7.40
7.80	0.52	0.68	5.3093	22.8000	20.3093	7.20
8.00	0.533333333	0.68	5.4323	23.0000	20.4323	7.00

8.20	0.546666667	0.68	5.5546	23.2000	20.5546	6.80
8.40	0.56	0.68	5.6764	23.4000	20.6764	6.60
8.60	0.573333333	0.67	5.7976	23.6000	20.7976	6.40
8.80	0.586666667	0.67	5.9182	23.8000	20.9182	6.20
9.00	0.6	0.67	6.0382	24.0000	21.0382	6.00
9.20	0.613333333	0.67	6.1576	24.2000	21.1576	5.80
9.40	0.626666667	0.67	6.2765	24.4000	21.2765	5.60
9.60	0.64	0.67	6.3948	24.6000	21.3948	5.40
9.80	0.653333333	0.66	6.5126	24.8000	21.5126	5.20
10.00	0.666666667	0.66	6.6298	25.0000	21.6298	5.00
10.20	0.68	0.66	6.7464	25.2000	21.7464	4.80
10.40	0.693333333	0.66	6.8625	25.4000	21.8625	4.60
10.60	0.706666667	0.66	6.9781	25.6000	21.9781	4.40
10.80	0.72	0.66	7.0931	25.8000	22.0931	4.20
11.00	0.733333333	0.66	7.2075	26.0000	22.2075	4.00
11.20	0.746666667	0.65	7.3215	26.2000	22.3215	3.80
11.40	0.76	0.65	7.4349	26.4000	22.4349	3.60
11.60	0.773333333	0.65	7.5478	26.6000	22.5478	3.40
11.80	0.786666667	0.65	7.6601	26.8000	22.6601	3.20
12.00	0.8	0.65	7.7720	27.0000	22.7720	3.00
12.20	0.813333333	0.65	7.8833	27.2000	22.8833	2.80
12.40	0.826666667	0.64	7.9941	27.4000	22.9941	2.60
12.60	0.84	0.64	8.1044	27.6000	23.1044	2.40
12.80	0.853333333	0.64	8.2142	27.8000	23.2142	2.20
13.00	0.866666667	0.64	8.3235	28.0000	23.3235	2.00
13.20	0.88	0.64	8.4323	28.2000	23.4323	1.80
13.40	0.893333333	0.64	8.5406	28.4000	23.5406	1.60
13.60	0.906666667	0.64	8.6484	28.6000	23.6484	1.40
13.80	0.92	0.63	8.7557	28.8000	23.7557	1.20
14.00	0.933333333	0.63	8.8625	29.0000	23.8625	1.00
14.20	0.946666667	0.63	8.9689	29.2000	23.9689	0.80
14.40	0.96	0.63	9.0748	29.4000	24.0748	0.60
14.60	0.973333333	0.63	9.1802	29.6000	24.1802	0.40
14.80	0.986666667	0.63	9.2851	29.8000	24.2851	0.20
15.00	1	0.63	9.3896	30.0000	24.3896	0.00
15.20	1.013333333	0.62	9.4936	30.2000	24.4936	-0.20
15.40	1.026666667	0.62	9.5971	30.4000	24.5971	-0.40
15.60	1.04	0.62	9.7002	30.6000	24.7002	-0.60
15.80	1.053333333	0.62	9.8028	30.8000	24.8028	-0.80
16.00	1.066666667	0.62	9.9050	31.0000	24.9050	-1.00
16.20	1.08	0.62	10.0067	31.2000	25.0067	-1.20
16.40	1.093333333	0.62	10.1080	31.4000	25.1080	-1.40
16.60	1.106666667	0.61	10.2088	31.6000	25.2088	-1.60
16.80	1.12	0.61	10.3092	31.8000	25.3092	-1.80
17.00	1.133333333	0.61	10.4091	32.0000	25.4091	-2.00
17.20	1.146666667	0.61	10.5086	32.2000	25.5086	-2.20
17.40	1.16	0.61	10.6077	32.4000	25.6077	-2.40
17.60	1.173333333	0.61	10.7063	32.6000	25.7063	-2.60
17.80	1.186666667	0.61	10.8046	32.8000	25.8046	-2.80

18.00	1.2	0.61	10.9024	33.0000	25.9024	-3.00
18.20	1.213333333	0.60	10.9997	33.2000	25.9997	-3.20
18.40	1.226666667	0.60	11.0967	33.4000	26.0967	-3.40
18.60	1.24	0.60	11.1932	33.6000	26.1932	-3.60
18.80	1.253333333	0.60	11.2893	33.8000	26.2893	-3.80
19.00	1.266666667	0.60	11.3851	34.0000	26.3851	-4.00
19.20	1.28	0.60	11.4804	34.2000	26.4804	-4.20
19.40	1.293333333	0.60	11.5753	34.4000	26.5753	-4.40
19.60	1.306666667	0.60	11.6698	34.6000	26.6698	-4.60
19.80	1.32	0.59	11.7639	34.8000	26.7639	-4.80
20.00	1.333333333	0.59	11.8576	35.0000	26.8576	-5.00
20.20	1.346666667	0.59	11.9509	35.2000	26.9509	-5.20
20.40	1.36	0.59	12.0438	35.4000	27.0438	-5.40
20.60	1.373333333	0.59	12.1363	35.6000	27.1363	-5.60
20.80	1.386666667	0.59	12.2284	35.8000	27.2284	-5.80
21.00	1.4	0.59	12.3202	36.0000	27.3202	-6.00
21.20	1.413333333	0.59	12.4115	36.2000	27.4115	-6.20
21.40	1.426666667	0.58	12.5025	36.4000	27.5025	-6.40
21.60	1.44	0.58	12.5931	36.6000	27.5931	-6.60
21.80	1.453333333	0.58	12.6833	36.8000	27.6833	-6.80
22.00	1.466666667	0.58	12.7732	37.0000	27.7732	-7.00
22.20	1.48	0.58	12.8627	37.2000	27.8627	-7.20
22.40	1.493333333	0.58	12.9518	37.4000	27.9518	-7.40
22.60	1.506666667	0.58	13.0405	37.6000	28.0405	-7.60
22.80	1.52	0.58	13.1289	37.8000	28.1289	-7.80
23.00	1.533333333	0.57	13.2169	38.0000	28.2169	-8.00
23.20	1.546666667	0.57	13.3046	38.2000	28.3046	-8.20
23.40	1.56	0.57	13.3919	38.4000	28.3919	-8.40
23.60	1.573333333	0.57	13.4788	38.6000	28.4788	-8.60
23.80	1.586666667	0.57	13.5654	38.8000	28.5654	-8.80
24.00	1.6	0.57	13.6517	39.0000	28.6517	-9.00
24.20	1.613333333	0.57	13.7376	39.2000	28.7376	-9.20
24.40	1.626666667	0.57	13.8231	39.4000	28.8231	-9.40
24.60	1.64	0.57	13.9083	39.6000	28.9083	-9.60
24.80	1.653333333	0.56	13.9932	39.8000	28.9932	-9.80
25.00	1.666666667	0.56	14.0777	40.0000	29.0777	-10.00
25.20	1.68	0.56	14.1619	40.2000	29.1619	-10.20
25.40	1.693333333	0.56	14.2457	40.4000	29.2457	-10.40
25.60	1.706666667	0.56	14.3292	40.6000	29.3292	-10.60
25.80	1.72	0.56	14.4124	40.8000	29.4124	-10.80
26.00	1.733333333	0.56	14.4952	41.0000	29.4952	-11.00
26.20	1.746666667	0.56	14.5777	41.2000	29.5777	-11.20
26.40	1.76	0.56	14.6599	41.4000	29.6599	-11.40
26.60	1.773333333	0.55	14.7418	41.6000	29.7418	-11.60
26.80	1.786666667	0.55	14.8233	41.8000	29.8233	-11.80
27.00	1.8	0.55	14.9045	42.0000	29.9045	-12.00
27.20	1.813333333	0.55	14.9854	42.2000	29.9854	-12.20
27.40	1.826666667	0.55	15.0660	42.4000	30.0660	-12.40
27.60	1.84	0.55	15.1463	42.6000	30.1463	-12.60

27.80	1.853333333	0.55	15.2262	42.8000	30.2262	-12.80
28.00	1.866666667	0.55	15.3059	43.0000	30.3059	-13.00
28.20	1.88	0.55	15.3852	43.2000	30.3852	-13.20
28.40	1.893333333	0.54	15.4642	43.4000	30.4642	-13.40
28.60	1.906666667	0.54	15.5429	43.6000	30.5429	-13.60
28.80	1.92	0.54	15.6213	43.8000	30.6213	-13.80
29.00	1.933333333	0.54	15.6994	44.0000	30.6994	-14.00
29.20	1.946666667	0.54	15.7773	44.2000	30.7773	-14.20
29.40	1.96	0.54	15.8548	44.4000	30.8548	-14.40
29.60	1.973333333	0.54	15.9320	44.6000	30.9320	-14.60
29.80	1.986666667	0.54	16.0089	44.8000	31.0089	-14.80
30.00	2	0.54	16.0855	45.0000	31.0855	-15.00

Refraction Calculation (Radial Component, Bicen)

*Without Optical box and cross slit

Wall Thickness (mm)	t	Fluid RI	n_f	Wall RI	n_w
2.5		1.33		1.49	

Inner Radius (mm)	R_i	Outer Radius (mm)	R_o	Cos θ_a
15		17.5		0.9659

r_a	C_f	r_f	Constant 1	Constant 2	Constant 3	Constant 4	θ_f	y_f
0.00	0.75	0.0000	0.0000	0.0000	0.0000	0.0000	0.0000	0.0000
0.20	0.75	0.1504	0.4952	0.4245	0.5548	0.6325	0.1484	0.1504
0.40	0.75	0.3008	0.9905	0.8490	1.1097	1.2651	0.2969	0.3007
0.60	0.75	0.4511	1.4859	1.2736	1.6647	1.8978	0.4454	0.4511
0.80	0.75	0.6015	1.9813	1.6982	2.2198	2.5307	0.5941	0.6015
1.00	0.75	0.7519	2.4769	2.1229	2.7751	3.1640	0.7429	0.7518
1.20	0.75	0.9023	2.9727	2.5477	3.3307	3.7977	0.8919	0.9021
1.40	0.75	1.0526	3.4687	2.9727	3.8866	4.4318	1.0412	1.0525
1.60	0.75	1.2030	3.9650	3.3979	4.4429	5.0664	1.1907	1.2027
1.80	0.75	1.3534	4.4616	3.8232	4.9996	5.7017	1.3405	1.3530
2.00	0.75	1.5038	4.9585	4.2487	5.5568	6.3377	1.4907	1.5033
2.20	0.75	1.6541	5.4558	4.6745	6.1145	6.9745	1.6413	1.6535
2.40	0.75	1.8045	5.9535	5.1005	6.6728	7.6121	1.7923	1.8036
2.60	0.75	1.9549	6.4516	5.5268	7.2317	8.2507	1.9438	1.9538
2.80	0.75	2.1053	6.9503	5.9535	7.7913	8.8904	2.0958	2.1039
3.00	0.75	2.2556	7.4494	6.3804	8.3516	9.5311	2.2484	2.2539
3.20	0.75	2.4060	7.9492	6.8077	8.9128	10.1730	2.4017	2.4039
3.40	0.75	2.5564	8.4495	7.2354	9.4748	10.8163	2.5555	2.5538

3.60	0.75	2.7068	8.9505	7.6635	10.0378	11.4609	2.7101	2.7037
3.80	0.75	2.8571	9.4522	8.0921	10.6017	12.1070	2.8654	2.8536
4.00	0.75	3.0075	9.9546	8.5210	11.1667	12.7547	3.0216	3.0033
4.20	0.75	3.1579	10.4578	8.9505	11.7328	13.4040	3.1785	3.1530
4.40	0.75	3.3083	10.9618	9.3805	12.3000	14.0551	3.3364	3.3027
4.60	0.75	3.4586	11.4667	9.8110	12.8685	14.7080	3.4953	3.4522
4.80	0.75	3.6090	11.9725	10.2421	13.4382	15.3629	3.6551	3.6017
5.00	0.75	3.7594	12.4792	10.6737	14.0093	16.0199	3.8160	3.7511
5.20	0.75	3.9098	12.9869	11.1060	14.5819	16.6791	3.9781	3.9004
5.40	0.75	4.0602	13.4957	11.5389	15.1559	17.3405	4.1413	4.0495
5.60	0.75	4.2105	14.0055	11.9725	15.7315	18.0043	4.3058	4.1986
5.80	0.75	4.3609	14.5165	12.4067	16.3087	18.6706	4.4716	4.3476
6.00	0.75	4.5113	15.0287	12.8417	16.8877	19.3395	4.6388	4.4965
6.20	0.75	4.6617	15.5420	13.2775	17.4684	20.0112	4.8074	4.6453
6.40	0.75	4.8120	16.0567	13.7140	18.0510	20.6858	4.9776	4.7939
6.60	0.75	4.9624	16.5727	14.1514	18.6355	21.3634	5.1493	4.9424
6.80	0.75	5.1128	17.0901	14.5896	19.2220	22.0442	5.3227	5.0907
7.00	0.75	5.2632	17.6090	15.0287	19.8106	22.7282	5.4979	5.2389
7.20	0.75	5.4135	18.1293	15.4686	20.4014	23.4157	5.6749	5.3870
7.40	0.75	5.5639	18.6512	15.9095	20.9945	24.1067	5.8539	5.5349
7.60	0.75	5.7143	19.1747	16.3514	21.5900	24.8015	6.0348	5.6826
7.80	0.75	5.8647	19.6998	16.7943	22.1879	25.5003	6.2179	5.8302
8.00	0.75	6.0150	20.2267	17.2382	22.7884	26.2031	6.4032	5.9775
8.20	0.75	6.1654	20.7554	17.6832	23.3915	26.9102	6.5909	6.1247
8.40	0.75	6.3158	21.2860	18.1293	23.9974	27.6217	6.7810	6.2716
8.60	0.75	6.4662	21.8184	18.5765	24.6061	28.3379	6.9737	6.4183
8.80	0.75	6.6165	22.3529	19.0249	25.2178	29.0590	7.1691	6.5648
9.00	0.7	6.7669	22.8894	19.4746	25.8327	29.7851	7.3673	6.7111

	5							
9.20	0.75	6.9173	23.4280	19.9254	26.4507	30.5166	7.5684	6.8570
9.40	0.75	7.0677	23.9688	20.3776	27.0721	31.2536	7.7727	7.0027
9.60	0.75	7.2180	24.5120	20.8311	27.6969	31.9963	7.9803	7.1481
9.80	0.75	7.3684	25.0574	21.2860	28.3253	32.7452	8.1914	7.2932
10.00	0.75	7.5188	25.6054	21.7422	28.9575	33.5004	8.4061	7.4380
10.20	0.75	7.6692	26.1558	22.2000	29.5935	34.2623	8.6246	7.5825
10.40	0.75	7.8195	26.7088	22.6592	30.2336	35.0311	8.8471	7.7265
10.60	0.75	7.9699	27.2646	23.1199	30.8779	35.8072	9.0739	7.8702
10.80	0.75	8.1203	27.8231	23.5823	31.5265	36.5910	9.3053	8.0134
11.00	0.75	8.2707	28.3846	24.0463	32.1797	37.3828	9.5413	8.1563
11.20	0.75	8.4211	28.9490	24.5120	32.8376	38.1831	9.7825	8.2986
11.40	0.75	8.5714	29.5165	24.9794	33.5004	38.9922	10.0289	8.4405
11.60	0.75	8.7218	30.0872	25.4486	34.1683	39.8107	10.2810	8.5818
11.80	0.75	8.8722	30.6612	25.9196	34.8416	40.6391	10.5392	8.7225
12.00	0.75	9.0226	31.2387	26.3925	35.5204	41.4779	10.8037	8.8626
12.20	0.75	9.1729	31.8197	26.8673	36.2050	42.3277	11.0751	9.0021
12.40	0.75	9.3233	32.4043	27.3442	36.8956	43.1892	11.3537	9.1409
12.60	0.75	9.4737	32.9928	27.8231	37.5925	44.0629	11.6401	9.2789
12.80	0.75	9.6241	33.5853	28.3042	38.2961	44.9498	11.9348	9.4160
13.00	0.75	9.7744	34.1818	28.7874	39.0065	45.8506	12.2385	9.5523
13.20	0.75	9.9248	34.7826	29.2729	39.7241	46.7662	12.5518	9.6876
13.40	0.75	10.0752	35.3878	29.7607	40.4493	47.6976	12.8755	9.8219
13.60	0.75	10.2256	35.9976	30.2508	41.1824	48.6460	13.2104	9.9550
13.80	0.75	10.3759	36.6121	30.7435	41.9238	49.6126	13.5575	10.0868
14.00	0.75	10.5263	37.2316	31.2387	42.6739	50.5988	13.9178	10.2173
14.20	0.75	10.6767	37.8562	31.7364	43.4331	51.6060	14.2926	10.3462
14.40	0.75	10.8271	38.4861	32.2369	44.2021	52.6362	14.6833	10.4735

14.60	0.75	10.9774	39.1216	32.7402	44.9812	53.6911	15.0914	10.5989
14.80	0.75	11.1278	39.7629	33.2463	45.7710	54.7732	15.5189	10.7221
15.00	0.75	11.2782	40.4102	33.7553	46.5721	55.8851	15.9678	10.8430
15.20	0.75	11.4286	41.0638	34.2674	47.3853	57.0297	16.4408	10.9613
15.40	0.75	11.5789	41.7239	34.7826	48.2113	58.2108	16.9408	11.0765
15.60	0.75	11.7293	42.3909	35.3011	49.0507	59.4325	17.4716	11.1882
15.80	0.75	11.8797	43.0651	35.8229	49.9046	60.7001	18.0376	11.2959
16.00	0.75	12.0301	43.7467	36.3482	50.7739	62.0197	18.6443	11.3988
16.20	0.75	12.1805	44.4363	36.8770	51.6597	63.3991	19.2987	11.4960
16.40	0.75	12.3308	45.1340	37.4095	52.5631	64.8484	20.0098	11.5865
16.60	0.75	12.4812	45.8404	37.9458	53.4855	66.3803	20.7894	11.6686
16.80	0.75	12.6316	46.5559	38.4861	54.4284	68.0123	21.6536	11.7402
17.00	0.75	12.7820	47.2809	39.0305	55.3936	69.7685	22.6254	11.7983
17.20	0.75	12.9323	48.0161	39.5790	56.3829	71.6847	23.7389	11.8381
17.40	0.75	13.0827	48.7618	40.1320	57.3986	73.8179	25.0491	11.8522
17.60	0.75	13.2331	49.5188	40.6895	58.4433	76.2687	26.6547	11.8268
17.80	0.75	13.3835	50.2877	41.2517	59.5199	79.2524	28.7685	11.7316
18.00	0.75	13.5338	51.0693	41.8188	60.6321	83.4623	32.0807	11.4672
18.20	0.75	13.6842	51.8642	42.3909	61.7841	#NUM!	#NUM!	#NUM!
18.40	0.75	13.8346	52.6735	42.9683	62.9809	#NUM!	#NUM!	#NUM!
18.60	0.75	13.9850	53.4980	43.5512	64.2289	#NUM!	#NUM!	#NUM!
18.80	0.75	14.1353	54.3389	44.1398	65.5360	#NUM!	#NUM!	#NUM!
19.00	0.75	14.2857	55.1974	44.7343	66.9122	#NUM!	#NUM!	#NUM!
19.20	0.75	14.4361	56.0748	45.3349	68.3707	#NUM!	#NUM!	#NUM!
19.40	0.75	14.5865	56.9726	45.9421	69.9295	#NUM!	#NUM!	#NUM!
19.60	0.75	14.7368	57.8926	46.5559	71.6142	#NUM!	#NUM!	#NUM!
19.80	0.75	14.8872	58.8368	47.1768	73.4633	#NUM!	#NUM!	#NUM!
20.0	0.7	15.037	59.8074	47.8050	75.5397	#NUM!	#NUM!	#NUM!

0	5	6						
20.20	0.75	15.1880	60.8072	48.4409	77.9605	#NUM!	#NUM!	#NUM!
20.40	0.75	15.3383	61.8392	49.0848	80.9996	#NUM!	#NUM!	#NUM!
20.60	0.75	15.4887	62.9072	49.7373	85.8440	#NUM!	#NUM!	#NUM!
20.80	0.75	15.6391	64.0156	50.3986	#NUM!	#NUM!	#NUM!	#NUM!
21.00	0.75	15.7895	65.1699	51.0693	#NUM!	#NUM!	#NUM!	#NUM!
21.20	0.75	15.9398	66.3768	51.7498	#NUM!	#NUM!	#NUM!	#NUM!
21.40	0.75	16.0902	67.6448	52.4407	#NUM!	#NUM!	#NUM!	#NUM!
21.60	0.75	16.2406	68.9851	53.1427	#NUM!	#NUM!	#NUM!	#NUM!
21.80	0.75	16.3910	70.4125	53.8563	#NUM!	#NUM!	#NUM!	#NUM!
22.00	0.75	16.5414	71.9477	54.5823	#NUM!	#NUM!	#NUM!	#NUM!
22.20	0.75	16.6917	73.6210	55.3215	#NUM!	#NUM!	#NUM!	#NUM!
22.40	0.75	16.8421	75.4802	56.0748	#NUM!	#NUM!	#NUM!	#NUM!
22.60	0.75	16.9925	77.6085	56.8430	#NUM!	#NUM!	#NUM!	#NUM!
22.80	0.75	17.1429	80.1797	57.6274	#NUM!	#NUM!	#NUM!	#NUM!
23.00	0.75	17.2932	83.7157	58.4290	#NUM!	#NUM!	#NUM!	#NUM!
23.20	0.75	17.4436	#NUM!	59.2494	#NUM!	#NUM!	#NUM!	#NUM!
23.40	0.75	17.5940	#NUM!	60.0900	#NUM!	#NUM!	#NUM!	#NUM!
23.60	0.75	17.7444	#NUM!	60.9526	#NUM!	#NUM!	#NUM!	#NUM!
23.80	0.75	17.8947	#NUM!	61.8392	#NUM!	#NUM!	#NUM!	#NUM!
24.00	0.75	18.0451	#NUM!	62.7523	#NUM!	#NUM!	#NUM!	#NUM!
24.20	0.75	18.1955	#NUM!	63.6945	#NUM!	#NUM!	#NUM!	#NUM!
24.40	0.75	18.3459	#NUM!	64.6692	#NUM!	#NUM!	#NUM!	#NUM!
24.60	0.75	18.4962	#NUM!	65.6802	#NUM!	#NUM!	#NUM!	#NUM!
24.80	0.75	18.6466	#NUM!	66.7324	#NUM!	#NUM!	#NUM!	#NUM!
25.00	0.75	18.7970	#NUM!	67.8316	#NUM!	#NUM!	#NUM!	#NUM!
25.20	0.75	18.9474	#NUM!	68.9851	#NUM!	#NUM!	#NUM!	#NUM!
25.40	0.75	19.0977	#NUM!	70.2026	#NUM!	#NUM!	#NUM!	#NUM!

25.60	0.75	19.2481	#NUM!	71.4965	#NUM!	#NUM!	#NUM!	#NUM!
25.80	0.75	19.3985	#NUM!	72.8844	#NUM!	#NUM!	#NUM!	#NUM!
26.00	0.75	19.5489	#NUM!	74.3913	#NUM!	#NUM!	#NUM!	#NUM!
26.20	0.75	19.6992	#NUM!	76.0557	#NUM!	#NUM!	#NUM!	#NUM!
26.40	0.75	19.8496	#NUM!	77.9427	#NUM!	#NUM!	#NUM!	#NUM!
26.60	0.75	20.0000	#NUM!	80.1797	#NUM!	#NUM!	#NUM!	#NUM!
26.80	0.75	20.1504	#NUM!	83.0995	#NUM!	#NUM!	#NUM!	#NUM!
27.00	0.75	20.3008	#NUM!	#NUM!	#NUM!	#NUM!	#NUM!	#NUM!
27.20	0.75	20.4511	#NUM!	#NUM!	#NUM!	#NUM!	#NUM!	#NUM!
27.40	0.75	20.6015	#NUM!	#NUM!	#NUM!	#NUM!	#NUM!	#NUM!
27.60	0.75	20.7519	#NUM!	#NUM!	#NUM!	#NUM!	#NUM!	#NUM!
27.80	0.75	20.9023	#NUM!	#NUM!	#NUM!	#NUM!	#NUM!	#NUM!
28.00	0.75	21.0526	#NUM!	#NUM!	#NUM!	#NUM!	#NUM!	#NUM!
28.20	0.75	21.2030	#NUM!	#NUM!	#NUM!	#NUM!	#NUM!	#NUM!
28.40	0.75	21.3534	#NUM!	#NUM!	#NUM!	#NUM!	#NUM!	#NUM!
28.60	0.75	21.5038	#NUM!	#NUM!	#NUM!	#NUM!	#NUM!	#NUM!
28.80	0.75	21.6541	#NUM!	#NUM!	#NUM!	#NUM!	#NUM!	#NUM!
29.00	0.75	21.8045	#NUM!	#NUM!	#NUM!	#NUM!	#NUM!	#NUM!
29.20	0.75	21.9549	#NUM!	#NUM!	#NUM!	#NUM!	#NUM!	#NUM!
29.40	0.75	22.1053	#NUM!	#NUM!	#NUM!	#NUM!	#NUM!	#NUM!
29.60	0.75	22.2556	#NUM!	#NUM!	#NUM!	#NUM!	#NUM!	#NUM!
29.80	0.75	22.4060	#NUM!	#NUM!	#NUM!	#NUM!	#NUM!	#NUM!
30.00	0.75	22.5564	#NUM!	#NUM!	#NUM!	#NUM!	#NUM!	#NUM!

*Error because angle between virtual point and true point of intersection point cannot be calculated.

Gantt Chart for first semester

No	Details	Week													
		1	2	3	4	5	6	7		8	9	10	11	12	13
1	Selection of Project Topic														
2	First meeting with my supervisor														
3	Preliminary Research work														
	a) Research the detail about laser Doppler anemometer (LDA)														
	b) Research on Teflon and refraction														
	c) Start designing the workbench using CATIA V5														
4	Preliminary Report preparation														
5	Submission of Preliminary Report (20 August 2010)														
6	Progress report preparation														
7	Submission of Progress Report (20 September 2010)														
8	Discussion and alteration of the design														
9	Design fabrication														
10	Seminar (20 September 2010)														
11	Submission of Interim Report Final Draft														
12	Oral Presentation preparation														
13	Oral Presentation (during study week)														

MID SEMESTER BREAK

Suggestion milestone Process

Figure: Gantt chart for first semester

Gantt Chart for second semester

No	Details	Week													
		1	2	3	4	5	6	7		8	9	10	11	12	13	14
	Assembly of the Test Section															
	Run leak test on the test section															
	Study of Refraction correction for LDA measurement															
	Drawing of laser beam refraction															
	Submission of progress report															
	Submission of FYP Abstract for SEDEX 28								MID SEMESTER							
	Experiment Using LDA on the Test Section															
	Poster Presentation															
	Pre-EDX															
	Submission of Dissertation and Technical paper															
	Oral Presentation															
	Submission of Final Report (Hard bound)															
									Process							

Figure: Gantt chart for first semester